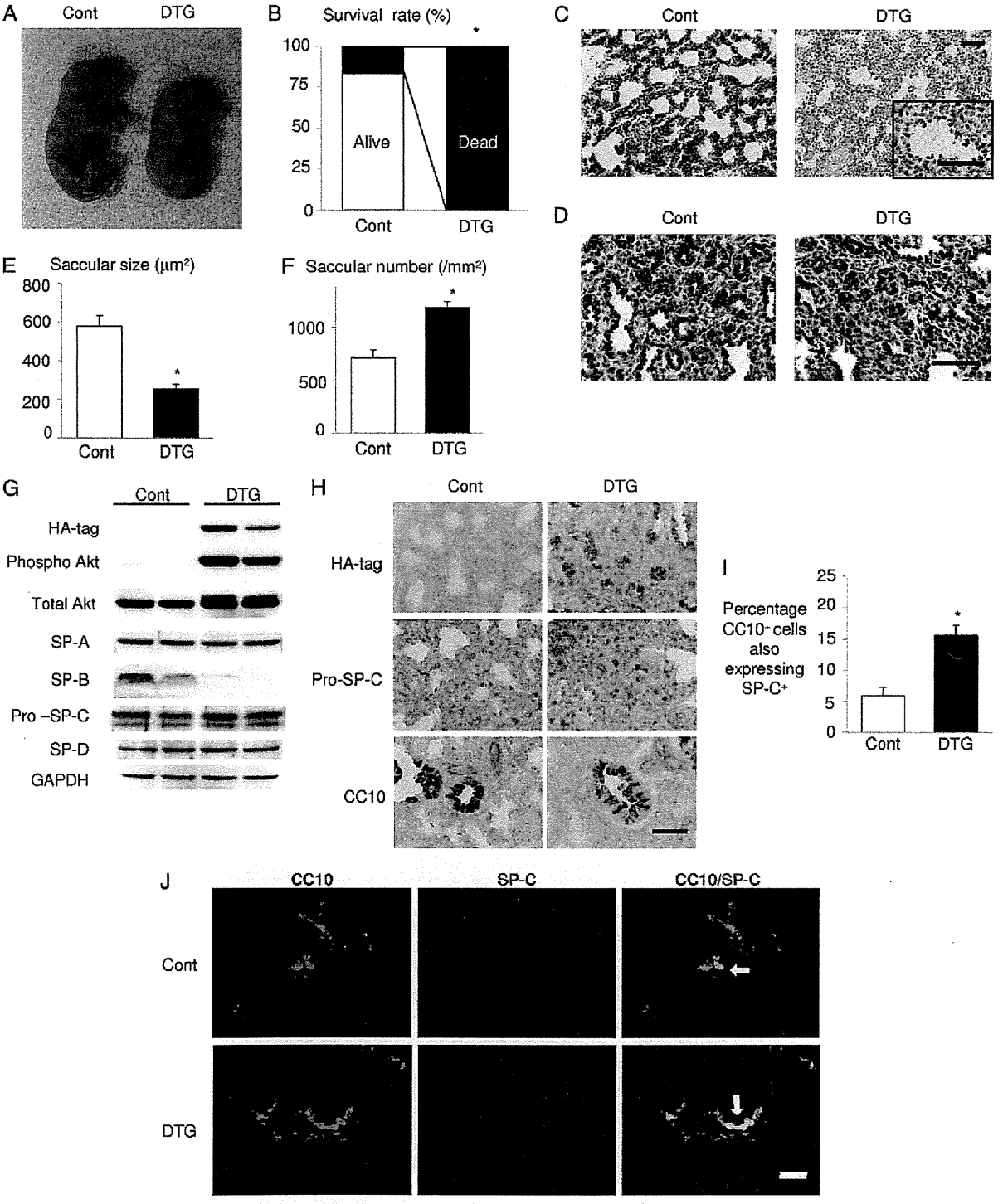


FIG. 4. Akt activation in lung epithelium results in RDS and lethality in preterm infants. (A) Gross appearance of infants. (B) Survival rate by 2 h after delivery. *, $P < 0.05$ ($n = 6$ control and $n = 5$ DTG mice from 2 dams). (C) HE staining of the lung sections of infants delivered by Caesarean section at E18.5. Scale bar, 50 μm. (D) PAS staining of the lung sections of infants delivered by Caesarean section at E18.5. Scale bar, 50 μm. (E) Saccular size at E18.5. *, $P < 0.05$ versus control. (F) Saccular number at E18.5. *, $P < 0.05$ versus control. For the experiments shown in panels E and F, $n = 3$ control and $n = 4$ DTG mice from 2 dams. (G) Western blot analysis of surfactant proteins (SP-A, SP-B, pro-SP-C, and SP-D). (H) Immunohistochemistry of HA tag (Akt1 transgene), pro-SP-C, and CC10 at E18.5. Scale bar, 50 μm. (I and J) Double immunostaining of CC10 and SP-C. CC10/SP-C double-positive cells are indicated by arrows. Scale bar, 100 μm. For both panels, $n = 4$ (Cont) and $n = 3$ (DTG) from 2 dams.

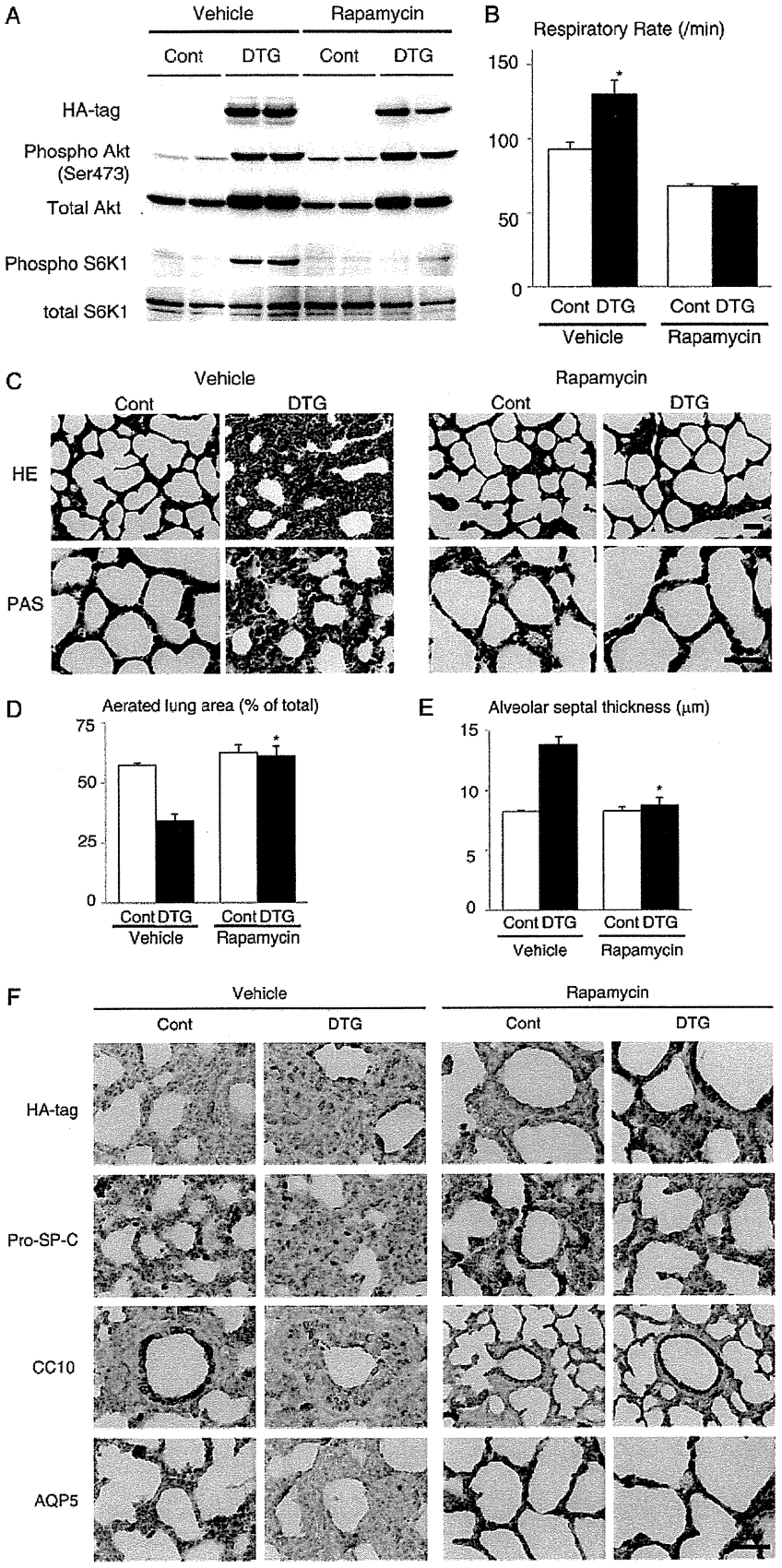
A
Vehicle
Rapamycin
Cont
DTG
Cont
DTG
HA-tag
Phospho Akt (Ser473)
Total Akt
Phospho S6K1
total S6K1
B
Respiratory Rate (/min)
150
100
50
0
Cont DTG
Cont DTG
Vehicle
Rapamycin
C
Vehicle
Rapamycin
Cont
DTG
Cont
DTG
HE
PAS
D
Aerated lung area (% of total)
75
50
25
0
Cont DTG
Cont DTG
Vehicle
Rapamycin
E
Alveolar septal thickness (μm)
15
10
5
0
Cont DTG
Cont DTG
Vehicle
Rapamycin
F
Vehicle
Rapamycin
Cont
DTG
Cont
DTG
HA-tag
Pro-SP-C
CC10
AQP5

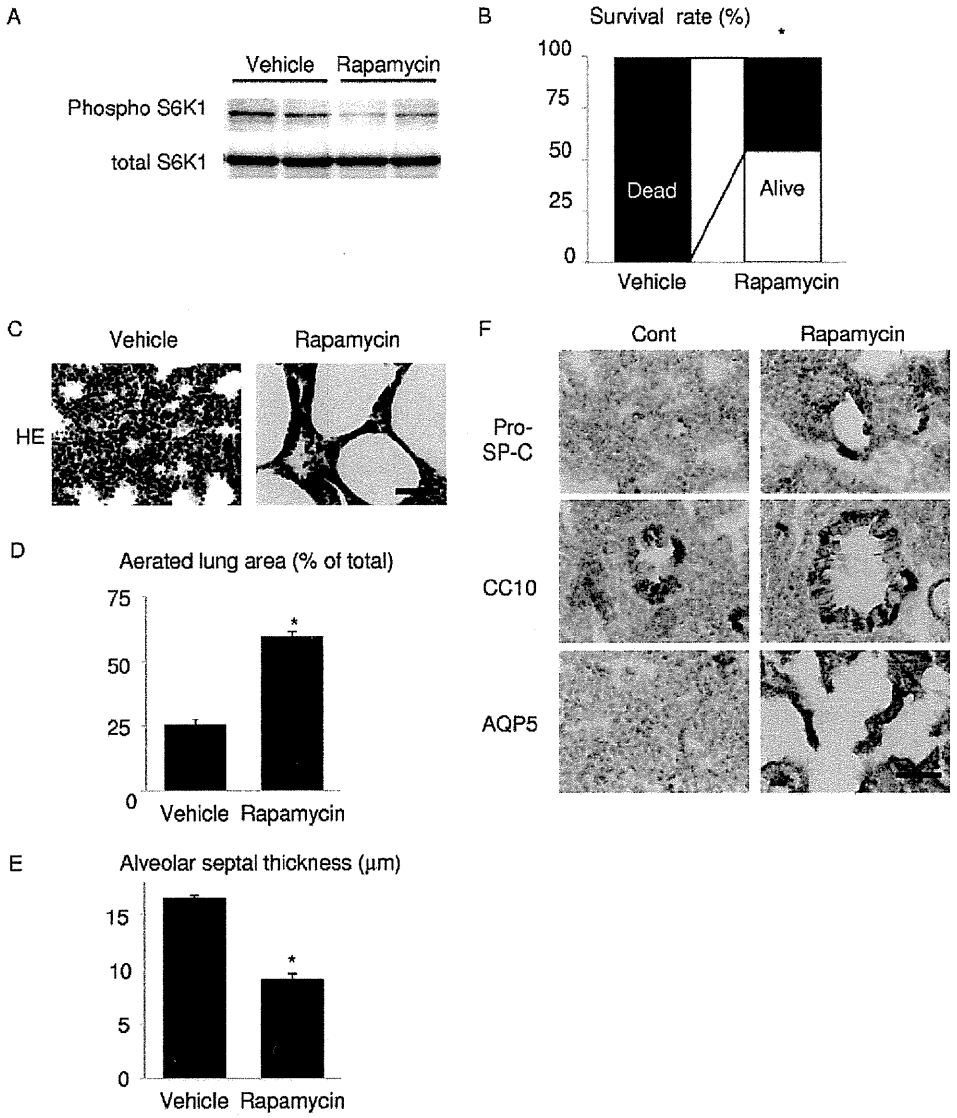


FIG. 6. Rapamycin improves respiratory distress and lung maturational defects induced by preterm delivery. (A) Western blot analysis of S6K1 in the lung. (B) Survival rate of wild-type pups 1 h after Caesarean section at E17.5. *, $P < 0.05$ versus vehicle-treated group. In the vehicle-treated group, $n = 15$ from a single dam. In the rapamycin group, $n = 24$ from 2 dams. (C) HE staining at 1 h after delivery. Scale bar, 50 μm. (D) Aerated lung area in vehicle- or rapamycin-treated pups. *, $P < 0.05$ versus vehicle-treated group. In the vehicle-treated group, $n = 3$ from a single dam; in the rapamycin group, $n = 4$ from 2 dams. (E) Thickness of alveolar septum in vehicle- or rapamycin-treated pups. *, $P < 0.05$ versus vehicle-treated group. In the vehicle-treated group, $n = 3$ from a single dam; in the rapamycin group, $n = 4$ from 2 dams. (F) Immunohistochemistry of pro-SP-C, CC10, and AQP5. Scale bar, 50 μm.

ing has a therapeutic potential for RDS induced by preterm delivery in wild-type mice.

**Activation of the Akt-mTOR pathway attenuates HIF-2-dependent VEGF expression in lung epithelial cells.** To investigate the mechanism by which Akt-mTOR signaling affects lung maturation, we examined the expression of VEGF, an angiogenic growth factor that is produced in the distal airway during late gestation and regulates coordinated development of alve-

FIG. 5. Rapamycin improves respiratory distress and lung maturational defects induced by Akt1 overexpression in lung epithelium. (A) Western blot analysis of Akt and S6K1 in the lung. (B) Respiratory rate of vehicle- or rapamycin-treated pups at P0. For vehicle experiments, $n = 7$ for both control and DTG mice from 3 dams; for rapamycin experiments, $n = 14$ (control) and $n = 11$ (DTG) mice from 4 dams. (C) Histological analysis. HE and PAS staining of lung sections at P0. Scale bar, 50 μm. (D) Aerated lung area in vehicle- or rapamycin-treated pups at P0. *, $P < 0.05$ versus vehicle-treated DTG mice. (E) Thickness of alveolar septum in vehicle- or rapamycin-treated pups at P0. *, $P < 0.05$ versus vehicle-treated DTG mice. For experiments shown in panels D and E, $n = 3$ control and $n = 3$ DTG vehicle-treated mice from 3 dams, and $n = 8$ control and $n = 7$ DTG rapamycin-treated mice from 4 dams. (F) Immunohistochemistry of HA tag, pro-SP-C, CC10, and AQP5 at P0. Scale bar, 50 μm.

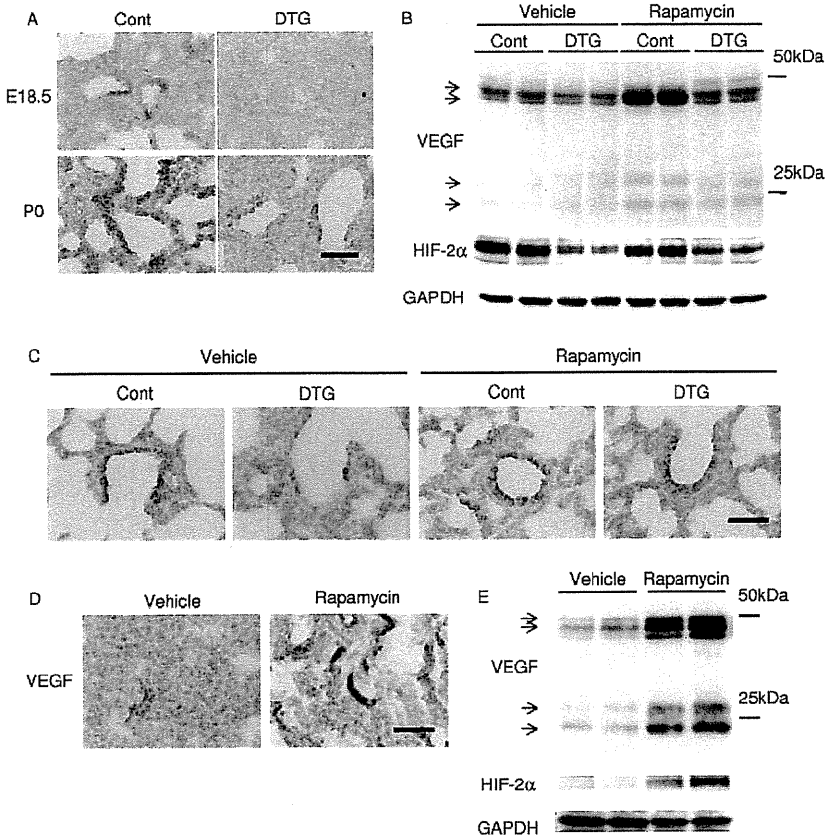


FIG. 7. Akt-mTOR pathway downregulates VEGF expression in the lung. (A) Immunostaining of VEGF at E18.5 and P0 in Akt1 TG mice. Scale bar, 50 μm. (B) Western blot analysis of VEGF and HIF-2α at P0 in Akt1 TG mice. (C) Immunostaining of VEGF at P0 in Akt1 TG mice. Scale bar, 50 μm. (D) Immunostaining of VEGF at E17.5 in wild-type mice. Scale bar, 50 μm. (E) Western blot analysis of VEGF and HIF-2α at E17.5 in wild-type mice.

olar epithelium and capillaries (4). Immunohistochemistry and Western blot analysis revealed that the expression levels of VEGF were downregulated in DTG mice both at E18.5 and P0 and were restored by rapamycin treatment (Fig. 7A to C). Since the expression of VEGF in the lung has been reported to depend on HIF-2 activity (4), we next examined the expression of HIF-2α protein in the lung. Western blot analysis revealed that the HIF-2α protein amount was downregulated in the lung of DTG mice (Fig. 7B). The expression levels of VEGF and HIF-2α were also examined in vehicle- or rapamycin-treated wild-type pups delivered at E17.5. Immunohistochemistry and Western blot analysis demonstrated the upregulation of VEGF and HIF-2α expression by rapamycin in wild-type mice delivered preterm (Fig. 7D and E). It was therefore concluded that activation of the Akt-mTOR pathway attenuates the expressions of VEGF and HIF-2α in the lung. However, it was also noted that the expression levels of HIF-2α do not necessarily correlate with those of VEGF because rapamycin treatment highly upregulated VEGF expression in control animals without altering HIF-2α expression levels (Fig. 7B, compare the vehicle control group and the rapamycin control group). We therefore examined whether Akt-mTOR signaling regulates the transcriptional activity of HIF-2. In cultured A549 lung epithelial cells, insulin induced downregulation of VEGF expression, which was reversed by rapamycin treatment (Fig. 8A). Luciferase assays using *VEGF-luc* as a reporter gene revealed that insulin attenuated transcriptional activity of HIF-2 on VEGF promoter, which was reversed by rapamycin treatment (Fig. 8B), while both insulin and rapamycin had minimal effects on HIF-1 transcriptional activity (Fig. 8C). These results suggest that activation of Akt-mTOR signaling attenuates HIF-2-dependent VEGF expression with respect to both the amount of HIF-2α protein and HIF-2 transcriptional activity.

**Activation of the Akt-mTOR pathway reduces alveolar capillary density.** To test whether Akt-mTOR-mediated downregulation of VEGF is associated with attenuated alveolar angiogenesis, vascular morphometry was performed in DTG and control mice at P0. Isolectin B4 staining revealed that alveolar capillary density was significantly reduced in DTG mice compared to that in control mice, and this reduction was rescued by rapamycin treatment (Fig. 9A and B). We also found that alveolar capillary density in wild-type mice delivered preterm at E17.5 was increased by rapamycin treatment (Fig. 9C and D). Thus, alveolar capillary density is closely linked to the level of VEGF expression in the lung. These results are consistent with our hypothesis that Akt-mTOR signaling promotes RDS through downregulation of VEGF.

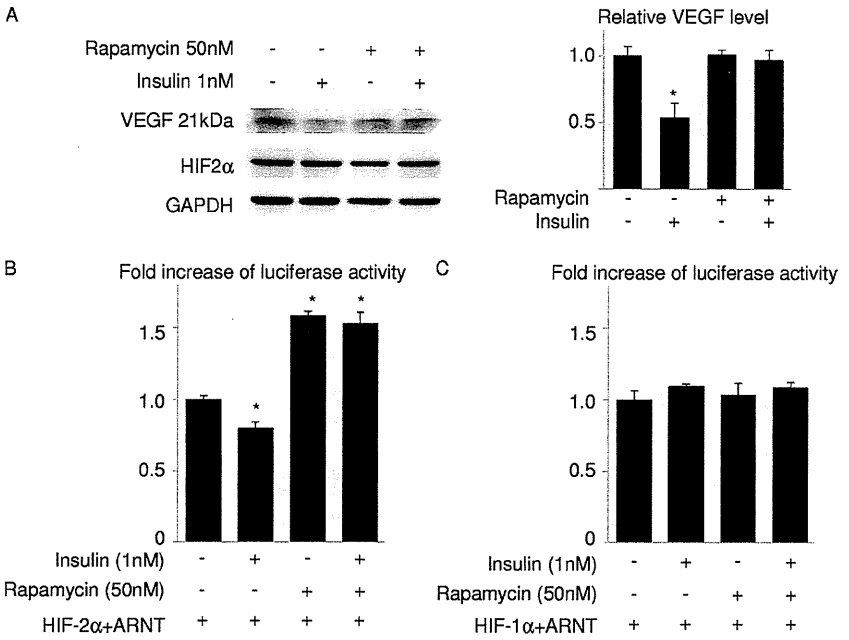


FIG. 8. Insulin attenuates VEGF expression and HIF-2 transcriptional activity on *VEGF* promoter in an mTOR-dependent manner in lung epithelial cells. (A) Western blot analysis of VEGF and HIF-2α in A549 cells treated with insulin and/or rapamycin for 48 h. The right panel shows the densitometric analysis. *, $P < 0.05$ versus the rapamycin (−)/insulin (−) group ($n = 3$ for each group). (B and C) Luciferase assays in A549 cells. A549 cells were transfected with a *VEGF-luc* reporter and expression vectors for HIF-1α, HIF-2α, and ARNT and treated with insulin and/or rapamycin. All experiments were performed in the presence of $CoCl_2$ to mimic hypoxic conditions. *, $P < 0.05$ versus the rapamycin (−)/insulin (−) group.

## DISCUSSION

In this study we have demonstrated that activation of Akt signaling in lung epithelial cells during embryogenesis results in transient respiratory difficulties in full-term infants and in RDS in preterm infants. These respiratory defects were associated with bronchiolar hyperplasia, expansion of CC10/SP-C double-positive cells, and impaired maturation of lung epithelial cells. We also found that Akt-mTOR signaling is critically involved in the pathogenesis of RDS because rapamycin treatment improved respiratory distress and lung maturational defects induced by Akt activation or preterm delivery. Mechanistically, Akt-mTOR signaling attenuates both the protein amounts and transcriptional activity of HIF-2, leading to downregulation of HIF-2-dependent expression of VEGF, an angiogenic growth factor that is required for maturation of alveolar epithelial cells. These observations suggest the possibility that aberrant activation of Akt-mTOR signaling or preterm delivery before the appropriate downregulation of this signaling axis plays a causal role in RDS through downregulation of HIF-2-dependent VEGF expression and that the mTOR-HIF-2 pathway may be a novel therapeutic target for infant RDS.

RDS is frequently observed in infants of diabetic mothers, and hyperactivation of insulin signaling in response to maternal hyperglycemia has been proposed to play a pathogenic role (19, 22). It was also previously shown that alveolar epithelium-specific deletion of *Pten* results in RDS, with approximately 90% of neonates dying within 2 h after birth (33). This phenotype of conditional *Pten* deletion is more severe than that of alveolar epithelium-specific Akt1 transgenic mice, suggesting the possibility that PI3K-dependent but Akt-independent pathways are also implicated in the occurrence of RDS. However, because another line of lung epithelium-specific *Pten* knockout mice generated by a similar method exhibit a very mild phenotype (i.e., lack of neonatal lethality, normal postnatal development, and mild bronchiolar hyperplasia) (7), the variation of phenotypes among different animal models may be due in part to the differences in the genetic background of the animals. Furthermore, rapamycin treatment of dams significantly improved the phenotype of alveolar epithelium-specific Akt1 transgenic mice. Taken together, these observations suggest that activation of the PI3K-Akt-mTOR pathway in lung epithelial cells *in utero* plays a causal role in the pathogenesis of RDS in infants with diabetic mothers.

Lung development in mice is histologically divided into four phases: the pseudoglandular stage (E9.5 to 16.5), canalicular stage (E16.5 to 17.5), terminal sac stage (E17.5 to P5), and alveolar stage (P5 to P30) (30). Differentiation of type I and type II epithelial cells and high levels of Pten expression in respiratory epithelium occur at the terminal sac stage (17), which is consistent with the idea that downregulation of the PI3K-Akt-mTOR pathway is required for epithelial differentiation. In humans, lung development is relatively advanced compared with that of mice, and the terminal sac stage corresponds to human preterm infants between 26 and 36 weeks of gestation, when a high complication rate of RDS is observed. Thus, inhibition of the PI3K-Akt-mTOR pathway at specific time points during a later stage of embryogenesis appears to be critical for normal lung development and maturation, and aberrant activation of Akt-mTOR signaling or preterm delivery

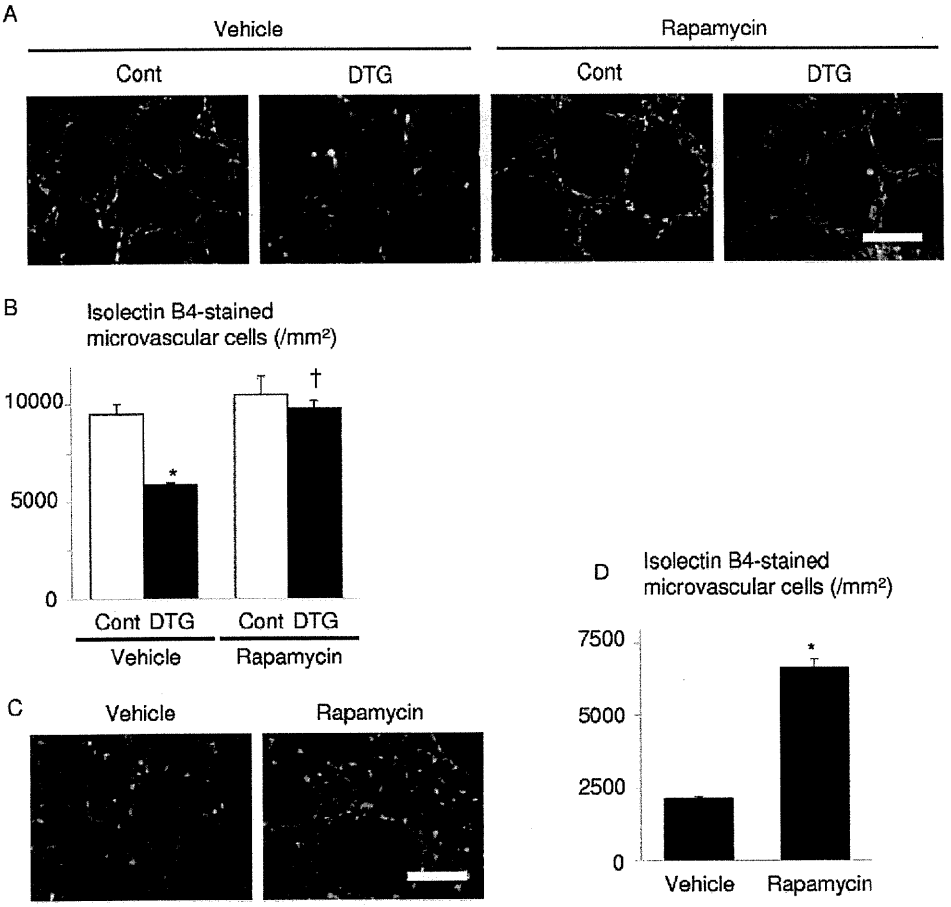


FIG. 9. Alveolar capillary bed formation is impaired by Akt1 overexpression in lung epithelium, which is improved by rapamycin administration to the dams. (A) Histological analysis of vehicle- or rapamycin-treated pups at P0. Sections were stained with isolectin B4-FITC conjugate (green) to detect endothelial cells and with wheat germ agglutinin-TRITC conjugate (red) for membrane staining. Scale bar, 50 μm. (B) Alveolar capillary density. *, $P < 0.05$ versus vehicle-treated control mice; †, $P < 0.05$ versus vehicle-treated DTG mice. In the vehicle-treated group, $n = 4$ control and $n = 3$ DTG mice from 2 dams; in the rapamycin group, $n = 4$ control and $n = 4$ DTG mice from 2 dams. (C) Histological analysis of vehicle- or rapamycin-treated wild-type pups born by Caesarean section at E17.5. Scale bar, 50 μm. (D) Alveolar capillary density. *, $P < 0.05$ versus vehicle-treated mice ($n = 4$ vehicle-treated mice from a single dam, and $n = 4$ rapamycin-treated mice from 2 dams).

before this signaling pathway is appropriately downregulated may result in the occurrence of RDS. The observation that rapamycin was effective for RDS also suggests that downregulation of mTOR signaling is sufficient to induce maturation of lung epithelial cells. Previous studies also implicated GATA6-Wnt/β-catenin signaling and calcineurin/nuclear factor of activated T cells (NFAT) signaling in lung maturation (6, 34). How these two signaling pathways and the PI3K-Akt-mTOR pathway coordinately regulate normal lung development remains to be investigated. It should also be noted that VEGF-induced angiogenesis is enhanced in the presence of rapamycin, which is inconsistent with the observation that VEGF induces endothelial cell proliferation via the Akt-mTOR pathway (32). This may be in part explained by the proangiogenic effects of the rapamycin-insensitive downstream effectors of Akt such as glycogen synthase kinase-3 and the FOXO family of transcription factors (1, 16).

Epithelial-endothelial interactions during lung development are critical in establishing a functional blood-gas interface, and normal lung function depends on the coordinated development of alveolar epithelium and capillaries, which is primarily regulated by VEGF (27). It was previously shown that deletion of HIF-2α in mice causes RDS due to downregulation of HIF-2-dependent VEGF expression in the lung (4). The similarity of the phenotypes between lung epithelium-specific Akt1 TG mice and HIF-2α-deficient mice prompted us to investigate the mechanistic link between mTOR and HIF-2. Previous studies showed that mTOR enhances the transcriptional activity of HIF-1 (13) and that VEGF expression in the heart is induced by activation of the Akt-mTOR pathway in TG mice in which the Akt1 transgene is inducible in the heart by doxycycline treatment (25), suggesting that mTOR promotes HIF-1-dependent VEGF expression. However, VEGF expression in the lung was downregulated by Akt1 overexpression and restored by rapamycin treatment. Consistently, HIF-2α expression levels were downregulated in the lung of DTG mice, and reporter gene assays in cultured lung epithelial cells revealed that insulin attenuates the transcriptional activity of HIF-2 on VEGF promoter in an mTOR-dependent manner. These results suggest the possibility that HIF-2 and VEGF are situated down-

stream of mTOR in the pathogenesis of RDS and that activation of the Akt-mTOR pathway in the lung leads to RDS through the downregulation of HIF-2-dependent VEGF expression. How mTOR differentially regulates the transcriptional activity of HIF-1 and HIF-2 awaits further investigation.

There are several limitations in this study. First, because the experiments to test whether overexpression of HIF-2 or VEGF in lung epithelium rescues the RDS phenotype of Akt1 TG mice were not performed, the direct link between the Akt-mTOR pathway and the HIF-2-VEGF pathway remains to be determined. Second, although it is highly possible that hyperactivation of insulin signaling plays a causal role in RDS (8, 10, 11), the present study does not provide definitive evidence showing that insulin signaling is, indeed, activated in lung epithelium of infants having a diabetic mother. It is also possible that other factors that activate the PI3K-Akt-mTOR pathway (e.g., insulin-like growth factors) may be involved in the pathogenesis of RDS. Third, the TG mouse system used in this study may activate Akt in the lung to a supra-physiological level that is not comparable to the level of Akt activation observed in infants of diabetic mothers.

In summary, the present study demonstrates a crucial role for the Akt-mTOR pathway in the pathogenesis of infant RDS and suggests that the mTOR-HIF-2 signaling axis is a novel therapeutic target for this disease state.

## ACKNOWLEDGMENTS

We thank S. L. McKnight for phEP-1, A. Ochiai and G. Ishii for A549 cells, and E. Fujita, R. Kobayashi, and Y. Ishiyama for technical assistance.

This work was supported by grants from the Ministry of Education, Culture, Sports, Science and Technology to I.K.

We declare that we have no conflicts of interest.

## REFERENCES

1. **Abid, M. R., et al.** 2004. Vascular endothelial growth factor activates PI3K/Akt/forkhead signaling in endothelial cells. Arterioscler. Thromb. Vasc. Biol. **24**:294–300.
2. **Bentley-Lewis, R., S. Levkoff, A. Stuebe, and E. W. Seely.** 2008. Gestational diabetes mellitus: postpartum opportunities for the diagnosis and prevention of type 2 diabetes mellitus. Nat. Clin. Pract. Endocrinol. Metab. **4**:552–558.
3. **Clausen, T. D., et al.** 2005. Poor pregnancy outcome in women with type 2 diabetes. Diabetes Care **28**:323–328.
4. **Compernolle, V., et al.** 2002. Loss of HIF-2α and inhibition of VEGF impair fetal lung maturation, whereas treatment with VEGF prevents fatal respiratory distress in premature mice. Nat. Med. **8**:702–710.
5. **Crowther, C. A., et al.** 2005. Effect of treatment of gestational diabetes mellitus on pregnancy outcomes. N. Engl. J. Med. **352**:2477–2486.
6. **Dave, V., et al.** 2006. Calcineurin/Nfat signaling is required for perinatal lung maturation and function. J. Clin. Invest. **116**:2597–2609.
7. **Dave, V., et al.** 2008. Conditional deletion of Pten causes bronchiolar hyperplasia. Am. J. Respir. Cell Mol. Biol. **38**:337–345.
8. **Dekowski, S. A., and J. M. Snyder.** 1992. Insulin regulation of messenger ribonucleic acid for the surfactant-associated proteins in human fetal lung in vitro. Endocrinology **131**:669–676.
9. **Feig, D. S., and V. A. Palda.** 2002. Type 2 diabetes in pregnancy: a growing concern. Lancet **359**:1690–1692.
10. **Guttentag, S. H., D. S. Phelps, W. Stenzel, J. B. Warshaw, and J. Floros.** 1992. Surfactant protein A expression is delayed in fetuses of streptozotocin-treated rats. Am. J. Physiol. **262**:L489–L494.
11. **Guttentag, S. H., D. S. Phelps, J. B. Warshaw, and J. Floros.** 1992. Delayed hydrophobic surfactant protein (SP-B, SP-C) expression in fetuses of streptozotocin-treated rats. Am. J. Respir. Cell Mol. Biol. **7**:190–197.
12. **Hallman, M., V. Glumoff, and M. Ramet.** 2001. Surfactant in respiratory distress syndrome and lung injury. Comp. Biochem. Physiol. Part A **129**:287–294.
13. **Hudson, C. C., et al.** 2002. Regulation of hypoxia-inducible factor 1α expression and function by the mammalian target of rapamycin. Mol. Cell. Biol. **22**:7004–7014.
14. **Jensen, D. M., et al.** 2004. Outcomes in type 1 diabetic pregnancies: a nationwide, population-based study. Diabetes Care **27**:2819–2823.
15. **Kim, C. F., et al.** 2005. Identification of bronchioalveolar stem cells in normal lung and lung cancer. Cell **121**:823–835.
16. **Kim, H. S., et al.** 2002. Regulation of angiogenesis by glycogen synthase kinase-3β. J. Biol. Chem. **277**:41888–41896.
17. **Luukko, K., A. Ylikorkala, M. Tiainen, and T. P. Makela.** 1999. Expression of LKB1 and PTEN tumor suppressor genes during mouse embryonic development. Mech. Dev. **83**:187–190.
18. **Maemura, K., et al.** 1999. Generation of a dominant-negative mutant of endothelial PAS domain protein 1 by deletion of a potent C-terminal transactivation domain. J. Biol. Chem. **274**:31565–31570.
19. **Montan, S., and S. Arulkumaran.** 2006. Neonatal respiratory distress syndrome. Lancet **367**:1878–1879.
20. **Morimoto, M., and R. Kopan.** 2009. rtTA toxicity limits the usefulness of the SP-C-rtTA transgenic mouse. Dev. Biol. **325**:171–178.
21. **Nold, J. L., and M. K. Georgieff.** 2004. Infants of diabetic mothers. Pediatr. Clin. North Am. **51**:619–637.
22. **Northway, W. H., Jr., R. C. Rosan, and D. Y. Porter.** 1967. Pulmonary disease following respirator therapy of hyaline-membrane disease. Bronchopulmonary dysplasia. N. Engl. J. Med. **276**:357–368.
23. **Perl, A. K., S. E. Wert, A. Nagy, C. G. Lobe, and J. A. Whitsett.** 2002. Early restriction of peripheral and proximal cell lineages during formation of the lung. Proc. Natl. Acad. Sci. U. S. A. **99**:10482–10487.
24. **Shioi, T., et al.** 2003. Rapamycin attenuates load-induced cardiac hypertrophy in mice. Circulation **107**:1664–1670.
25. **Shiojima, I., et al.** 2005. Disruption of coordinated cardiac hypertrophy and angiogenesis contributes to the transition to heart failure. J. Clin. Invest. **115**:2108–2118.
26. **Shiojima, I., et al.** 2002. Akt signaling mediates postnatal heart growth in response to insulin and nutritional status. J. Biol. Chem. **277**:37670–37677.
27. **Stenmark, K. R., and S. H. Abman.** 2005. Lung vascular development: implications for the pathogenesis of bronchopulmonary dysplasia. Annu. Rev. Physiol. **67**:623–661.
28. **Taniguchi, C. M., B. Emanuelli, and C. R. Kahn.** 2006. Critical nodes in signalling pathways: insights into insulin action. Nat. Rev. Mol. Cell Biol. **7**:85–96.
29. **Tichelaar, J. W., W. Lu, and J. A. Whitsett.** 2000. Conditional expression of fibroblast growth factor-7 in the developing and mature lung. J. Biol. Chem. **275**:11858–11864.
30. **Warburton, D., et al.** 2000. The molecular basis of lung morphogenesis. Mech. Dev. **92**:55–81.
31. **Whitsett, J. A., and T. E. Weaver.** 2002. Hydrophobic surfactant proteins in lung function and disease. N. Engl. J. Med. **347**:2141–2148.
32. **Xue, Q., et al.** 2009. Rapamycin inhibition of the Akt/mTOR pathway blocks select stages of VEGF-A164-driven angiogenesis, in part by blocking S6Kinase. Arterioscler. Thromb. Vasc. Biol. **29**:1172–1178.
33. **Yanagi, S., et al.** 2007. Pten controls lung morphogenesis, bronchioalveolar stem cells, and onset of lung adenocarcinomas in mice. J. Clin. Invest. **117**:2929–2940.
34. **Zhang, Y., et al.** 2008. A Gata6-Wnt pathway required for epithelial stem cell development and airway regeneration. Nat. Genet. **40**:862–870.

# Ryanodine Receptor Type 2 Is Required for the Development of Pressure Overload-Induced Cardiac Hypertrophy

Yunzeng Zou, Yanyan Liang, Hui Gong, Ning Zhou, Hong Ma, Aili Guan, Aijun Sun, Ping Wang, Yuhong Niu, Hong Jiang, Hiroyuki Takano, Haruhiro Toko, Atsushi Yao, Hiroshi Takeshima, Hiroshi Akazawa, Ichiro Shiojima, Yuqi Wang, Issei Komuro, Junbo Ge

***Abstract***—Ryanodine receptor type 2 (RyR-2) mediates $Ca^{2+}$ release from sarcoplasmic reticulum and contributes to myocardial contractile function. However, the role of RyR-2 in the development of cardiac hypertrophy is not completely understood. Here, mice with or without reduction of *RyR-2* gene (*RyR-2*$^{+/-}$ and wild-type, respectively) were analyzed. At baseline, there was no difference in morphology of cardiomyocyte and heart and cardiac contractility between *RyR-2*$^{+/-}$ and wild-type mice, although $Ca^{2+}$ release from sarcoplasmic reticulum was impaired in isolated *RyR-2*$^{+/-}$ cardiomyocytes. During a 3-week period of pressure overload, which was induced by constriction of transverse aorta, isolated *RyR-2*$^{+/-}$ cardiomyocytes displayed more reduction of $Ca^{2+}$ transient amplitude, rate of an increase in intracellular $Ca^{2+}$ concentration during systole, and percentile of fractional shortening, and hearts of *RyR-2*$^{+/-}$ mice displayed less compensated hypertrophy, fibrosis, and contractility; more apoptosis with less autophagy of cardiomyocytes; and similar decrease of angiogenesis as compared with wild-type ones. Moreover, constriction of transverse aorta-induced increases in the activation of calcineurin, extracellular signal-regulated protein kinases, and protein kinase B/Akt but not that of $Ca^{2+}$/calmodulin-dependent protein kinase II, and its downstream targets in the heart of wild-type mice were abolished in the *RyR-2*$^{+/-}$ one, suggesting that RyR-2 is a regulator of calcineurin, extracellular signal-regulated protein kinases, and Akt but not of calmodulin-dependent protein kinase II activation during pressure overload. Taken together, our data indicate that RyR-2 contributes to the development of cardiac hypertrophy and adaptation of cardiac function during pressure overload through regulation of the sarcoplasmic reticulum $Ca^{2+}$ release; activation of calcineurin, extracellular signal-regulated protein kinases, and Akt; and cardiomyocyte survival. (***Hypertension.*** **2011;58:1099-1110.)** • **Online Data Supplement**

**Key Words:** $Ca^{2+}$ ■ calcineurin ■ cardiac hypertrophy ■ pressure overload ■ ryanodine receptor

Cardiac hypertrophy is usually a compensatory response of the heart to hemodynamic overload, including hypertension, valve diseases, and myocardial infarction.[1] At the beginning, cardiac hypertrophy has beneficial effects on maintaining cardiac output by reducing wall stress. Prolonged hypertrophy, however, may eventually lead to heart failure (HF).[1] Development of cardiac hypertrophy and HF is a complex process involving many aspects of alterations, such as abnormality of intracellular $Ca^{2+}$ homeostasis, activation of a variety of protein kinases, reprogramming of specific gene expression, disorders of metabolism, and so forth.[2] Among these alterations, abnormality of intracellular $Ca^{2+}$ homeostasis is a critical one.[3,4]

Intracellular $Ca^{2+}$ homeostasis is regulated by $Ca^{2+}$ handling proteins, which control cardiomyocyte function, including excitation-contraction (E-C) coupling of cardiomyocytes.[5,6] Voltage-dependent L-type $Ca^{2+}$ channels (LCC) activated by membrane depolarization allow $Ca^{2+}$ entry into the cell, triggering a $Ca^{2+}$-induced $Ca^{2+}$ release (CICR) from sarcoplasmic reticulum (SR) through a ryanodine type 2 receptor (RyR-2) and muscle contraction. Elevated cytosolic $Ca^{2+}$ is then removed from the cytosol for relaxation, which

Received March 21, 2011; first decision April 6, 2011; revision accepted September 14, 2011.

From the Shanghai Institute of Cardiovascular Diseases, Zhongshan Hospital (Y.Z., Y.L., N.Z., A.G., A.S., Y.N., H.J., J.G.) and Institutes of Biomedical Sciences (H.G.), Fudan University, Shanghai, China; Department of Vascular Surgery (Y.W.), Zhongshan Hospital, Fudan University, Shanghai, China; Department of Cardiology (H.M.), Second Affiliated Hospital, Zhejiang University College of Medicine, Hangzhou, China; Department of Cardiovascular Science and Medicine (P.W., H.Taka., H.To.), Chiba University Graduate School of Medicine, Chiba, Japan; Department of Cardiovascular Medicine (H.A., I.S., I.K.), Osaka University Graduate School of Medicine, Osaka, Japan; Department of Cardiovascular Medicine (A.Y.), University of Tokyo Graduate School of Medicine, Tokyo, Japan; Department of Biochemistry (H.Take.), Tohoku University Graduate School of Medicine, Sendai, Japan.

The first six authors contributed equally to this work.

Correspondence to Yunzeng Zou or Junbo Ge, Shanghai Institute of Cardiovascular Diseases, Zhongshan Hospital, Fudan University, 180 Feng Lin Rd, Shanghai 200032, China (E-mail zou.yunzeng@zs-hospital.sh.cn or jbge@zs-hospital.sh.cn); or Issei Komuro, Department of Cardiovascular Medicine, Osaka University Graduate School of Medicine, 2-2 Yamadaoka, Suita, Osaka 565-0871, Japan (E-mail komuro-tky@umin.ac.jp).



*Hypertension* **is available at http://hyper.ahajournals.org** **DOI: 10.1161/HYPERTENSIONAHA.111.173500**

is mediated by several pathways involving uptake to SR by SR $Ca^{2+}$-ATPase 2 (SERCA2), uptake to mitochondria by $Ca^{2+}$ uniport, and extrusion from the cell by $Na^{+}/Ca^{2+}$ exchanger (NCX).[7]

Alterations in $Ca^{2+}$ handling proteins, such as RyR-2, LCC, SERCA2, and NCX, not only induce abnormality of CICR but also associate with cardiac hypertrophy and HF.[7–15] Because RyR-2 is a major CICR channel, it might greatly regulate the development of cardiac hypertrophy. FK506-binding protein (FKBP) 12.6 is a regulatory protein that tightly binds to RyR-2 and stabilizes the channel.[16,17] Numerous lines of clinical and experimental evidence have indicated that altered RyR-2 gene and function contribute to cardiac disorders, including catecholaminergic polymorphic ventricular tachycardia or arrhythmogenic right ventricular cardiomyopathy type 2,[15] cardiac hypertrophy, and dysfunction.[18,19] Furthermore, RyR-2 is hyperphosphorylated by protein kinase A (PKA) in HF, resulting in dissociation of FKBP12.6 from RyR-2 and $Ca^{2+}$ leaks from SR in diastole, which impair contractility.[16,17] Thus, alteration in RyR-2 is critically involved in abnormality of $Ca^{2+}$ handling and contractile dysfunction in HF. However, the role of RyR-2 in the development of cardiac hypertrophy, especially in the pressure overload-induced one, is still not completely understood.

Moreover, because intracellular $Ca^{2+}$ concentration cyclically alters during each heartbeat, it is assumed that there exist specialized microdomains where $Ca^{2+}$ functions as a signaling molecule independent of E-C coupling.[20] How $Ca^{2+}$ enters into these potential microdomains in response to hypertrophic stimuli remains unknown, although inositol 1,4,5-triphosphate receptors, T-type $Ca^{2+}$ channels, and transient receptor potential channels have been suggested as possible sources of E-C coupling-independent $Ca^{2+}$ entry.[21] In addition, $Ca^{2+}$ activates 2 major $Ca^{2+}$-dependent hypertrophic signaling pathways, the $Ca^{2+}$/calmodulin-dependent protein kinase II (CaMKII)-histone deacetylase (HDAC) pathway and the calcineurin (CnA)-nuclear factor of activated T cells (NFAT) pathway. CaMKII induces phosphorylation and nuclear export of HDAC, leading to the relief of HDAC-mediated transcriptional repression of myocyte enhancer factor 2 (MEF2) and MEF2-dependent transcription of hypertrophic genes.[22] CnA dephosphorylates NFAT, which leads to nuclear translocation of NFAT and upregulation of NFAT-dependent transcription of hypertrophic genes such as *atrial natriuretic peptide* (*ANP*) and *GATA binding protein 4* (*GATA4*).[23] Although CaMKII has been indicated to phosphorylate and activate RyR-2,[24] there is no direct evidence showing the relationship between RyR-2 and CaMKII or CnA, especially during the development of cardiac hypertrophy after pressure overload.

Additionally, we have reported previously that CnA regulates cardiomyocyte hypertrophy induced by isoproterenol through activation of extracellular signal-regulated kinases (ERKs), a critical regulator of cell growth.[25] Protein kinase B/Akt is also known to be upregulated in response to pressure overload and implicated in the development of load-induced cardiac hypertrophy. The present study was, therefore, designed to elucidate the effects of *RyR-2* reduction on the development of hemodynamic overload-induced cardiac hypertrophy and the relative mechanisms.

## Methods

An expanded Methods section is available in the online Data Supplement (please see http://hyper.ahajournals.org).

### Mice

Generation of *RyR-2* mutant mice (C57B/L6 strain), identification of the mutation, and induction of pressure overload in 12-week–old male mice by thoracic aorta constriction (TAC) have been described previously.[24,26,27] The mice were housed in a room with a 12-hour light/dark cycle and allowed free access to food and water. All of the animal protocols were approved by the Fudan University Animal Care and Use Committee and complied with Guidelines for the Care and Use of Laboratory Animals published by the National Academy Press (National Institutes of Health Publication No. 85-23, revised 1996).

### Echocardiography and Catheterization Measurement

Transthoracic echocardiography was performed by using an animal-specific instrument (Visual Sonics Vevo770, Visual Sonics Inc).[27,28] Mice were anesthetized with isoflurane, and M-mode images of the left ventricle (LV) were recorded when the heart rate of the mice was maintained at 450 to 500 bpm by changing isoflurane concentrations from 0.5% to 4.0% according to heart rate.[28] Hemodynamic parameters such as blood pressure (BP) and left ventricular (LV) end-diastolic pressure were measured by a 1.4 F cardiac catheter (Millar Instruments, Inc) connected to a Mac Laboratory system (AD Instruments).

### Isolation of Adult Cardiomyocytes and Intracellular $Ca^{2+}$ Measurement

Adult cardiomyocytes were isolated from mice by Langendorff perfusion method, and intracellular $Ca^{2+}$ concentration was measured by use of fluo-3, as described previously.[29]

### Histological Analyses

Cardiomyocyte hypertrophy and extent of LV fibrosis were measured in hematoxylin and eosin and van Gieson stained LV sections, respectively.[27,30] The density of capillaries in LV section was examined by CD31 immunostaining.[27] Apoptosis and autophagy of cardiomyocytes were detected in situ by costaining $\alpha$-major histocompatibility complex in paraffin-embedded heart tissue sections.

### Northern Blotting

Total RNA (10 $\mu$g) extracted from LV tissues was size fractionated in 1.2% formaldehyde agarose gels and transferred to nylon membranes. The blots were hybridized with the [$\alpha$-$^{32}$P]dCTP (Du Point-New England Nuclear Co)-labeled cDNA fragments.[30]

### Western Blotting

Western blot methods were used to examine the protein expression or phosphorylation of ERKs, Akt1, CaMII, CnA, RyR-2, poly (ADP-ribose) polymerase-1, and Beclin1. Phosphorylation sites recognized by antiphosphor-Ark1 and CaMKII antibodies are Ser473 and Thr286, respectively. For detection of phosphorylation of CnA, total protein (500 $\mu$g) of the LV tissue was immunoprecipated by an anti-CnA antibody.

### Statistical Analysis

All of the values are expressed as mean±SD of >3 experiments. Values of $P<0.05$ were considered statistically significant.

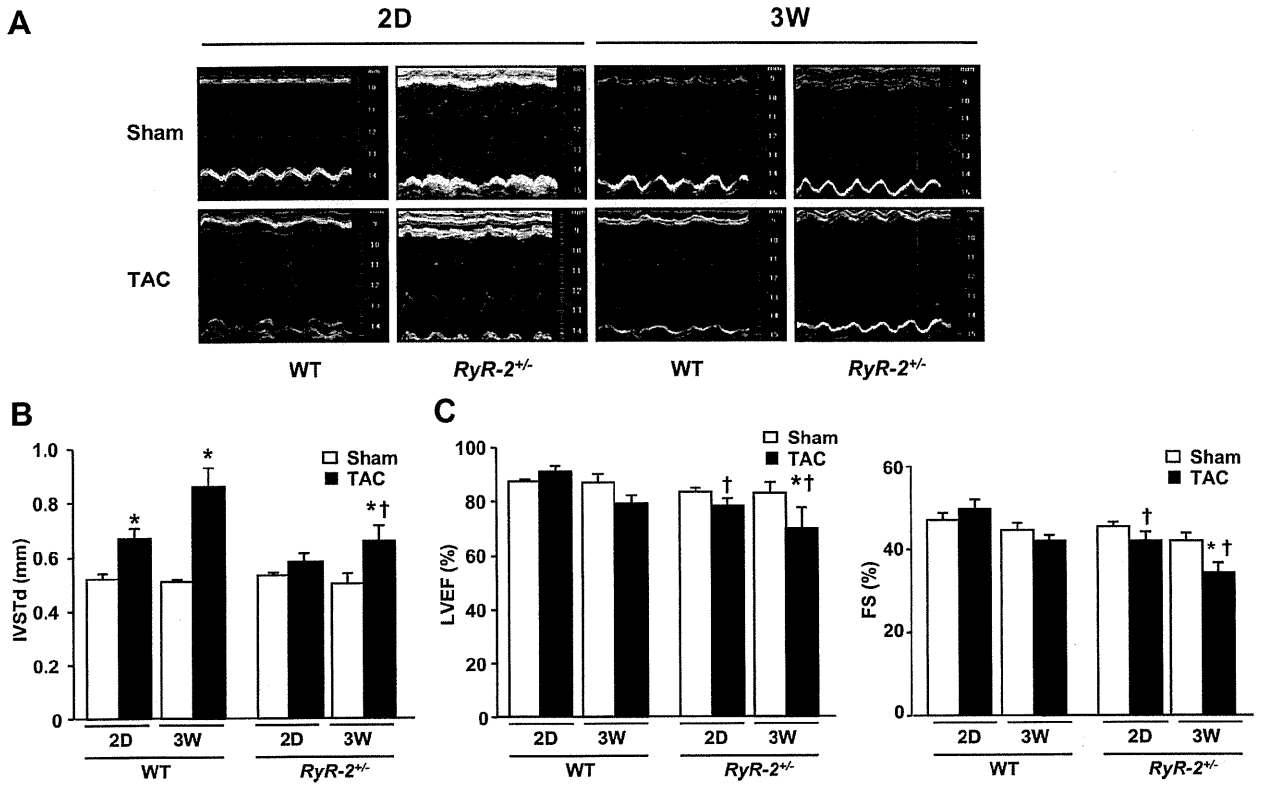


**Figure 1.** Echocardiographic studies 2 days (2D) and 3 weeks (3W) after sham or thoracic aorta constriction (TAC) operation. **A**, M-mode tracings. Representative photographs are shown. **B** and **C**, Wall thickness, ejection fraction (EF), and fractional shortening (FS) of left ventricle (LV). IVSTd indicates thickness of interventricular septum at diastole. Data represent mean±SD of 5 to 12 mice. *$P<0.05$ vs respective sham; †$P<0.05$ vs corresponding wild-type (WT)-TAC.

## Results

### Altered $Ca^{2+}$ Handling in Adult Cardiomyocytes of *RyR-2*$^{-/-}$ Mice

We first examined the impact of heterozygous disruption of the *RyR-2* gene on $Ca^{2+}$ handling and contractility in isolated adult cardiomyocytes (Table S1, please see http://hyper.ahajournals.org). At basal condition, $Ca^{2+}$ transient amplitude, the rate of an increase in intracellular $Ca^{2+}$ concentration during systole, and percentile of fractional shortening were significantly reduced in *RyR-2*$^{+/-}$ cardiomyocytes compared with wild-type (WT) ones, although the half-time of relaxation from caffeine-induced contracture (half-time of diastole phase) was comparable between them. At 3 weeks after TAC, $Ca^{2+}$ transient amplitude, rate of an increase in intracellular $Ca^{2+}$ concentration during systole of systolic phase, and percentile of fractional shortening were significantly reduced both in WT and *RyR-2*$^{+/-}$ cardiomyocytes, whereas half-time of diastole phase was extended in WT but not in *RyR-2*$^{+/-}$ cardiomyocytes. However, the reduction of $Ca^{2+}$ transient amplitude, rate of an increase in intracellular $Ca^{2+}$ concentration during systole, and percentile of fractional shortening after TAC in *RyR-2*$^{+/-}$ cardiomyocytes were more than in WT ones. On the other hand, the addition of ryanodine resulted in a significant decrease of the percentile of fractional shortening in WT cardiomyocytes but only a slight reduction in *RyR-2*$^{+/-}$ cardiomyocytes (Table S2).

### Attenuated Cardiac Hypertrophy and Contractility in *RyR-2*$^{-/-}$ Mice in Response to Pressure Overload

There was no significant difference in cardiac dimension and contractility evaluated by echocardiography between sham-operated WT and *RyR-2*$^{+/-}$ mice (Figure 1 and Table). At 2 days after TAC, a time point without efficient compensation of LV hypertrophy under hemodynamic overload, although there was a slight difference in cardiac hypertrophy between the 2 types of mice, LV dysfunctions characterized by LV ejection fraction, LV fractional shortening, LV end-diastolic pressure, and LV pressure increase and decay (dP/dt) were significantly impaired in *RyR-2*$^{+/-}$ mice compared with WT mice. At 3 weeks after TAC, thickness of interventricular septum in diastole and LV contractility in *RyR-2*$^{+/-}$ mice were both significantly reduced compared with those in WT mice, and hemodynamic studies showed the increased LV end-diastolic pressure and decreased peak dP/dt ($dP/dt_{max}$) in *RyR-2*$^{+/-}$ mice compared with WT mice. Heart weight/body weight ratio of *RyR-2*$^{+/-}$ mice 3 weeks after TAC was significantly smaller than that of WT mice (Table), and histological analysis revealed that heart size and cross-sectional area of cardiomyocytes were significantly reduced in *RyR-2*$^{+/-}$ mice compared with WT mice (Figure 2A and 2B). The examination of isolated cardiomyocytes also confirmed that the surface area of isolated cardiomyocytes was significantly reduced in *RyR-2*$^{+/-}$ cells compared with WT

**Table. Biometric, Echocardiographic, and Hemodynamic Parameters at 2 d and 3 wk After Sham and TAC Operation**

| | WT | | | | *RyR-2*$^{+/-}$ | | | |
|---|---|---|---|---|---|---|---|---|
| Mice TAC | Sham-2d | TAC-2d | Sham-3W | TAC-3W | Sham-2d | TAC-2d | Sham-3W | TAC-3W |
| n | 5 | 5 | 10 | 13 | 5 | 5 | 9 | 10 |
| BP, mm Hg | 93.0±11.0 | 153.0±14.0* | 90.0±12.0 | 156.0±18.0* | 89.0±13.0 | 150.0±17.0* | 87.0±7.0 | 139.0±25.0* |
| BW, g | 23.4±2.8 | 23.9±2.2 | 23.8±2.4 | 24.0±2.3 | 23.7±2.8 | 23.8±2.6 | 22.3±1.5 | 23.5±2.0 |
| HW, mg | 112.5±10.8 | 135.0±9.3* | 118.3±15.1 | 227.2±37.3* | 113.5±9.5 | 125.4±9.2 | 115.0±17.0 | 160.0±29.0*† |
| HW/BW, mg/g | 4.8±2.1 | 5.8±1.0* | 4.9±0.8 | 9.1±1.3* | 4.8±1.7 | 5.3±1.4 | 4.9±0.5 | 6.4±1.1*† |
| LVDs, mm | 1.75±0.35 | 1.55±0.42* | 1.77±0.32 | 1.85±0.35 | 1.77±0.55 | 1.80±0.36† | 1.79±0.34 | 2.03±0.31*† |
| LVDd, mm | 3.38±0.45 | 3.40±0.32 | 3.43±0.35 | 3.96±0.52 | 3.40±0.30 | 3.48±0.35 | 3.25±0.45 | 3.81±0.31* |
| LVEDP, mm Hg | 3.5±0.6 | 3.0±1.5 | 4.0±0.5 | 7.2±2.0* | 4.5±1.0 | 8.0±2.5† | 5.0±1.2 | 15.2±4.2*† |
| $dP/dt_{max}$, mm Hg | 2120±300 | 2670±310* | 2140±160 | 4090±250* | 2060±320 | 2150±260† | 2010±300 | 2230±347† |
| $dP/d_{min}$, mm Hg | 2010±280 | 2520±250* | 2070±90 | 3750±320* | 1880±230 | 2080±200† | 1800±300 | 2015±327† |

Adult male WT and *RyR-2*$^{+/-}$ mice were operated with sham or TAC. Two d (2d) or 3 wk (3W) later, analyses of biometry, echocardiography, and hemodynamics were performed. BW indicates body weight; BP, systolic blood pressure; HW, heart weight; HW/BW, HW:BW ratio; LV, left ventricular; LVDs, LV dimension in systole; LVDd, LV dimension in diastole; LVEDP, LV end-diastolic pressure; $dP/dt_{max}$ and $dP/dt_{min}$, maximal rates of LV pressure increase and decay; TAC, thoracic aorta constriction; WT, wild-type; RyR-2, ryanodine receptor type 2.

*$P<0.05$ vs respective sham.

†$P<0.05$ vs corresponding WT with TAC.

cells after TAC, although they were comparable between the 2 types of cells at baseline (Figure 2C). The extent of myocardial fibrosis evaluated by histology, Western blot analysis for collagen I$\alpha$ expression in LV tissue, and growth of isolated cardiac fibroblasts was significantly reduced in *RyR-2*$^{+/-}$ mice compared with WT mice (Figure 3). There was no significant difference in these parameters between WT and *RyR-2*$^{+/-}$ mice at baseline.

## Alteration of Hemodynamic Load-Responsive Gene Expression Program

Induction of fetal-type cardiac genes is one of the hypertrophic responses of the heart. We examined the expression of *ANP*, *brain natriuretic peptide* (*BNP*), and *skeletal* $\alpha$*-actin* ($\alpha$*-SKA*) genes in the heart after TAC. TAC-mediated induction of *ANP* and *BNP* genes was downregulated, whereas induction of the $\alpha$*-SKA* gene was not altered at day 2 and enhanced 3 weeks after TAC in the heart of *RyR-2*$^{+/-}$ mice (Figure 4).

The expression of genes encoding $Ca^{2+}$ handling proteins is also responsive to hemodynamic load. We, therefore, examined the expression of *SERCA2*, *LCC*, and *NCX* genes, as well as *RyR-2* genes, in the heart after TAC. In WT hearts, 3 weeks of pressure overload induced downregulation of *RyR-2* and *SERCA2* genes and upregulation of *LCC* and *NCX* genes. However, in *RyR-2*$^{+/-}$ hearts, the expression levels of *SERCA2* and *LCC* genes were not altered, whereas the *NCX* gene was downregulated (Figure 5A through 5E).

We also assessed the effects of the reduction of the *RyR-2* gene on protein expression and phosphorylation state of the receptor. The changes of RyR-2 protein were similar to those of the *RyR-2* gene (Figure 5F). RyR-2 function is affected by its binding proteins, such as FKBP 12.6 and PKA.[15–17,21,24] We, thus, examined the binding of these 2 proteins with RyR-2 in WT and *RyR-2*$^{+/-}$ mice (Figure S1). The amount of FKBP12.6-associated RyR-2 was less in the *RyR-2*$^{+/-}$ heart compared with the WT, whereas PKA-phosphorylated RyR-2 in the *RyR-2*$^{+/-}$ heart was more than the WT heart under basal condition, suggesting that an upregulation of RyR-2 phosphorylation compensated for RyR-2 deficiency. TAC for 3 weeks decreased the amount of FKBP12.6-associated RyR-2 not only in WT mice but also in *RyR-2*$^{+/-}$ mice. However, TAC-increased PKA phosphorylation of RyR-2 in the *RyR-2*$^{+/-}$ heart was more than in the WT heart.

## Attenuated Activation of Hypertrophic Signaling Pathways in Response to Pressure Overload in *RyR-2*$^{-/-}$ Mice

Because pressure overload-induced cardiac hypertrophy is attenuated in *RyR-2*$^{+/-}$ mice, we examined whether the load-induced activation of hypertrophic signaling pathways[31] is impaired in *RyR-2*$^{+/-}$ hearts. CaMKII and CnA are critical regulators of $Ca^{2+}$-mediated cardiac hypertrophy, and pressure overload activated these 2 proteins (Figure 6A and 6B) and their respective target molecules, HDACs/MEF2 and GATA4 (Figure S2A and S2B) in WT hearts. However, activation of CnA and expression of *GATA4* mRNA in response to pressure overload were impaired in *RyR-2*$^{+/-}$ hearts, whereas the activation of CaMKII and HDACs and expression of the *MEF2* gene were comparable between WT and *RyR-2*$^{+/-}$ hearts. To ask whether the changes of activation of CaMKII and CnA were because of the changes in their protein expression, we examined the expression of total CaMKII and CnA proteins in LV tissues (Figure 6A and 6B). Although CaMKII protein was only slightly increased in both types of mice at 3 weeks after TAC, CnA protein was similarly increased in the 2 mice, suggesting that the increases in cardiac CaMKII phosphorylation in both types of mice and the decrease of CnA phosphorylation in *RyR-2*$^{+/-}$ mice after 3 weeks of TAC are not because of the changes of CaMKII and CnA protein expression. Signaling pathways mediated by ERK1/2 and Akt are also known to be upregulated in response to pressure overload and implicated in the development of load-induced cardiac hyper-

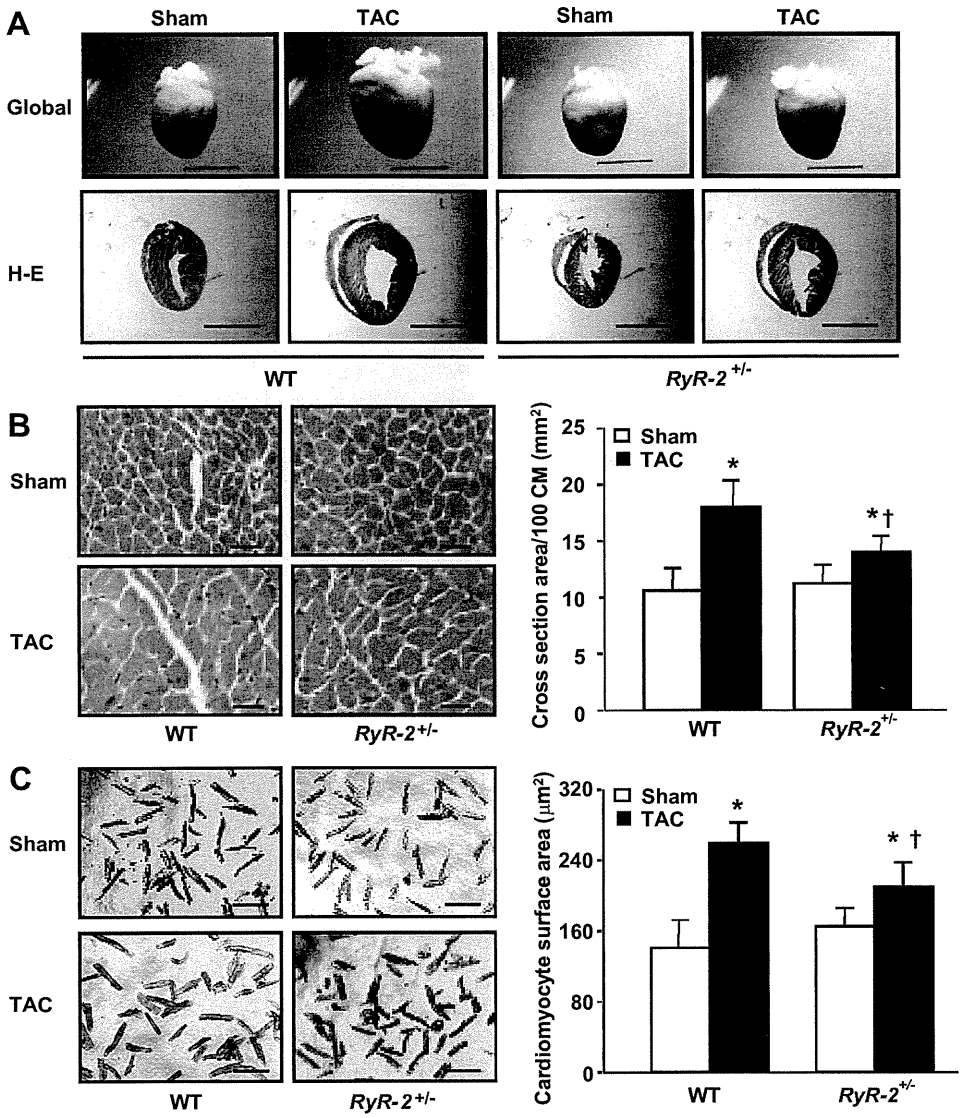


**Figure 2.** Cardiac hypertrophy at 2 days (2D) and 3 weeks (3W) after sham or thoracic aorta constriction (TAC) operation. **A,** Representative photographs of global hearts (top) and hematoxylin/eosin (H-E) staining of longitudinal heart sections (bottom). Scale bar, 2.5 mm. **B,** Representative photomicrographs illustrating left ventricular (LV) cardiomyocyte cross-sections. Scale bar, 25 μm. Measurements of cross-sectional area were performed in 10 points from 1 LV section (100 cardiomyocytes from 1 point), and 5 LV sections from 1 heart were measured. Data represent mean±SD of 5 to 12 hearts. **C,** Representative photomicrographs of isolated cardiomyocytes. Scale bar, 50 μm. The surface area of cardiomyocytes was measured in 100 cells per mouse. Data represent mean±SD from 3 mice. *$P<0.05$ vs respective sham; †$P<0.05$ vs corresponding wild-type (WT)-TAC.

trophy. TAC for 3 weeks induced robust activation of ERK1/2 and Akt in WT hearts but not in *RyR-2*$^{+/-}$ hearts (Figure 6C and 6D). Also, activities of p70$^{S6}$ kinase, a downstream molecule of Akt1, were consistent with phosphorylation of Akt1 (Figure S3).

## Increased Apoptosis, Decreased Autophagy, and Unchanged Angiogenesis in Pressure-Overloaded Heart

Although heterozygous deletion of the *RyR-2* gene led to abnormal $Ca^{2+}$ homeostasis and contractility in isolated cardiomyocytes, contractile function in vivo was not altered in *RyR-2*$^{+/-}$ mice, indicating that the alteration in $Ca^{2+}$ handling is compensated in in vivo situation. Nonetheless, contractile function was significantly reduced in *RyR-2*$^{+/-}$ mice compared with WT mice after pressure overload. This suggests that there exist additional mechanisms that contribute to impaired cardiac function in *RyR-2*$^{+/-}$ mice independent of the alteration in $Ca^{2+}$ homeostasis.

Apoptosis of cardiomyocytes is a well-established mediator of HF.[27,32] Although the number of apoptotic cardiomyocytes was comparable between WT and *RyR-2*$^{+/-}$ mice at baseline condition, apoptotic cells in the *RyR-2*$^{+/-}$ heart were significantly increased compared with those in the WT heart after chronic pressure overload (Figure 7A). The amount of cleaved poly (ADP-ribose) polymerase 1, another marker of apoptosis, was also increased in the *RyR-2*$^{+/-}$ heart compared with the WT heart (Figure 7B). Thus, heterozygous deletion of the *RyR-2* gene led to increased apoptosis of cardiomyocytes after chronic pressure overload.

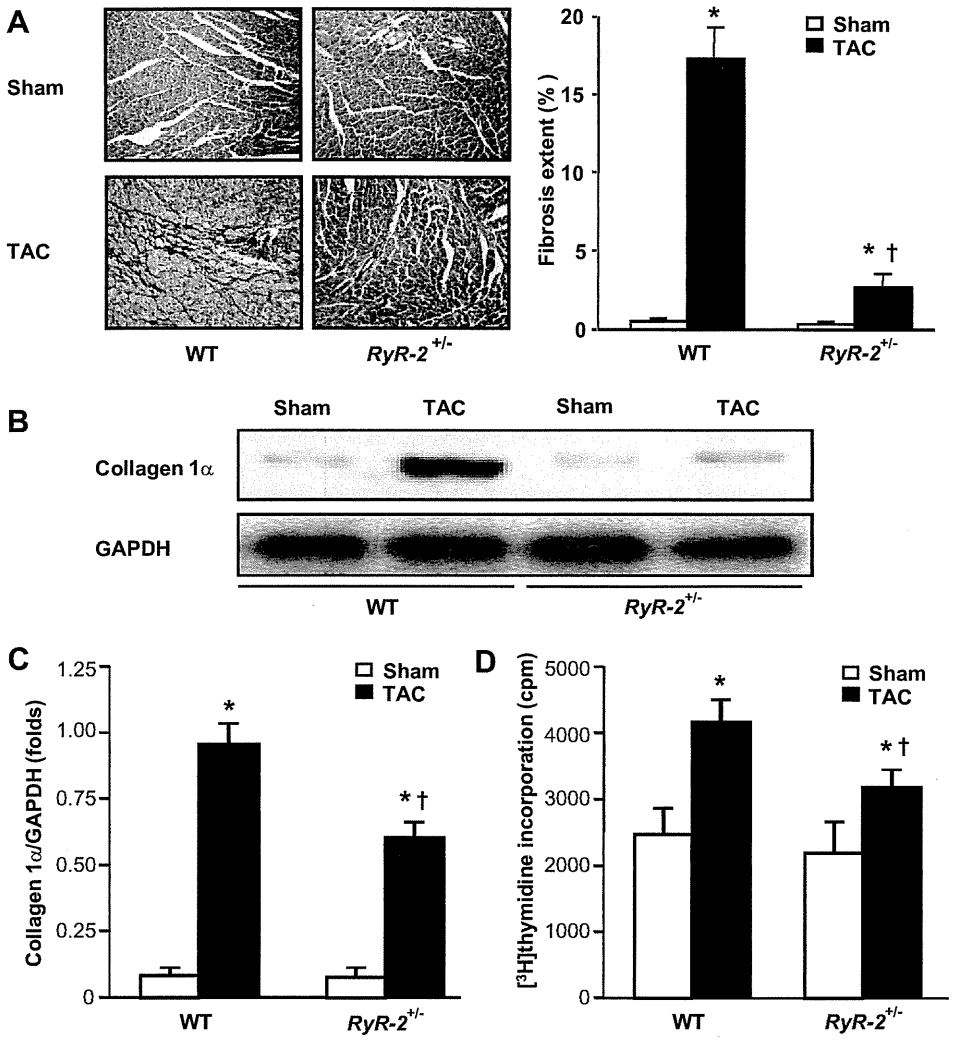


**Figure 3.** Analyses for myocardial fibrosis 3 weeks after sham or thoracic aorta constriction (TAC). **A**, Representative photomicrographs of van-Gieson–stained left ventricular (LV) sections. Fibrosis area was measured in 8 fields from 1 LV section and 5 sections from 1 heart. **B** and **C**, Western blot analysis for collagen 1α protein expression. GAPDH was served as a loading control. The intensities of collagen 1α were quantitated as folds of GAPDH. Data represent mean±SD from 6 hearts. **D**, DNA synthesis in isolated cardiac fibroblasts. DNA synthesis was evaluated by measuring the incorporation of [$^3$H]thymidine into the cultured fibroblasts. Data represent mean±SD from 3 mice. *$P$<0.05 vs respective sham; †$P$<0.05 vs corresponding WT-TAC.

Although the role of autophagy in the pathogenesis of HF is controversial, autophagy of cardiomyocytes appears to be an adaptive response to the increased cardiac workload, at least in some situations.[33,34] Immunostaining and Western blot analysis revealed that the extent of autophagy after pressure overload, as evidenced by LC3b-positive dots or increased expression of beclin1, was attenuated in *RyR-2*$^{+/-}$ hearts compared with WT hearts (Figure 7C and 7D), indicating that heterozygous deletion of the *RyR-2* gene led to decreased autophagy in the heart after pressure overload.

Myocardial ischemia induced by impaired coronary angiogenesis is another critical mediator of contractile dysfunction.[27,35,36] In the present study, however, the number of capillaries and the expression of vascular endothelial growth factor were not altered between WT and *RyR-2*$^{+/-}$ hearts after chronic pressure overload (Figure 8), suggesting that myocardial ischemia does not specifically contribute to contractile dysfunction in *RyR-2*$^{+/-}$ hearts.

## Discussion

RyR-2 mediates $Ca^{2+}$ release from the SR and plays a central role in the regulation of $Ca^{2+}$ homeostasis and contractility in cardiac myocytes.[6,17] In the present study, we have demonstrated that RyR-2 also plays a critical role in the development of cardiac hypertrophy and hypertrophic responses of the heart.

It was reported previously that homozygous deletion of the *RyR-2* gene resulted in embryonic lethality at approximately embryonic day 10, with morphological abnormalities of the heart.[26] In *RyR-2*$^{+/-}$ mice, there was no apparent cardiac phenotype at baseline, as evidenced by echocardiography, hemodynamic studies, and histological analyses. However, abnormal $Ca^{2+}$ release from the SR and reduced contractility were observed in isolated adult cardiomyocytes obtained from *RyR-2*$^{+/-}$ mice. This indicates that a defect in $Ca^{2+}$ handling at the single cell level is compensated in *RyR-2*$^{+/-}$ mice at the organ level. The expression levels of $Ca^{2+}$

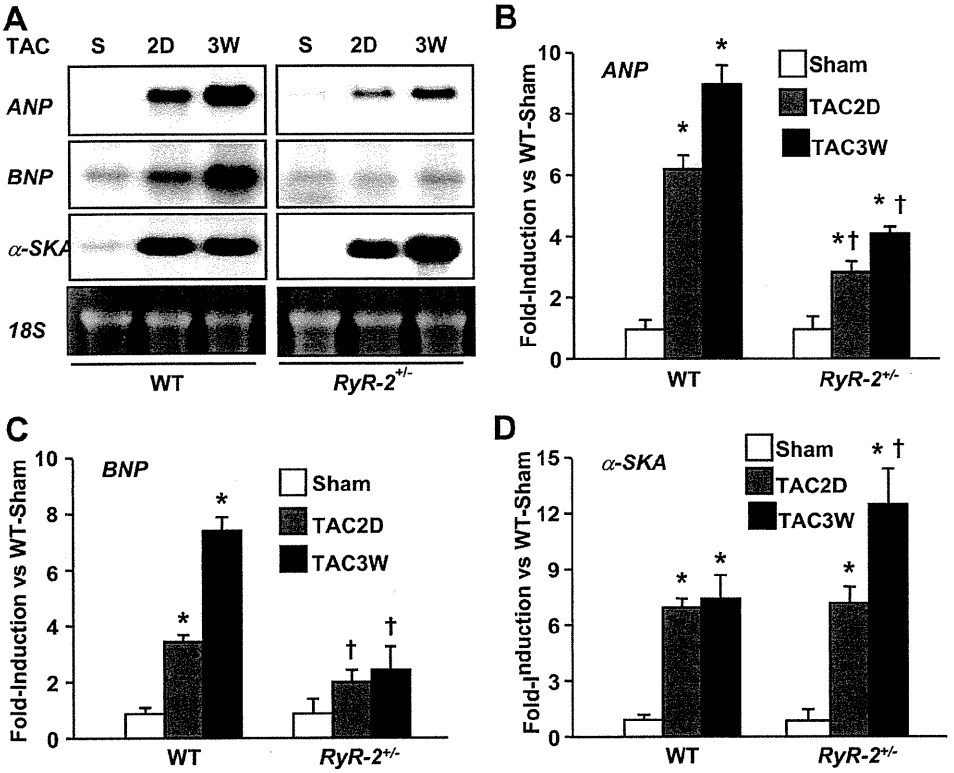


**Figure 4.** Expression of fetal-type cardiac genes. **A**, Representative Northern blots. Thoracic aorta constriction (TAC) 2D and TAC3W represent 2 days and 3 weeks after TAC, respectively. Expression levels of *ANP*, *BNP*, and *α-SKA* genes were analyzed by measuring the intensities and expressed as percentage of those obtained from wild-type (WT)-sham. Data represent mean±SD from 3 hearts. **P*<0.05 vs respective sham; †*P*<0.05 vs corresponding WT-TAC.

handling proteins (SERCA2, LCC, and NCX) other than RyR-2 were not altered between WT and *RyR-2*$^{+/-}$ mice at baseline. Although the exact nature of this compensation is unknown at present, there are 2 possibilities that might contribute to the compensation. At first, activation of the sympathetic nervous system because of the decrease of RyR-2 might enhance the in vivo cardiac performance at baseline. The second could be attributed to the in vivo hyperphosphorylation and upregulation of the function of RyR-2 because of the decrease of the receptor. Our data showing the increases in association of RyR-2 with PKA and dissociation of FKBP12.6 from the receptor in the heart of *RyR-2*$^{+/-}$ mice at baseline provide evidence for this explanation.

It has been known that RyR-2 is downregulated and hyperphosphorylated in HF.[17] We also observed that the degree of downregulation of the RyR-2 gene and protein was associated with the degree of heart dysfunction in mice. Furthermore, we have shown that *RyR-2*$^{+/-}$ mice exhibited impaired contractility in response to pressure overload both at the early and late stages, indicating that RyR-2 is required for the maintenance of contractile function under hemodynamic stress. One explanation for this is that a compensatory mechanism that maintains the contractile function of *RyR-2*$^{+/-}$ heart in vivo is disrupted by extensive overload, leading to the impairment of contractile function in *RyR-2*$^{+/-}$ mice under hemodynamic stress. An alternative and not mutually exclusive explanation is that there exist additional mechanisms that contribute to the contractile dysfunction of *RyR-2*$^{+/-}$ mice independent of the alteration in $Ca^{2+}$ handling. One possible $Ca^{2+}$-independent mechanism of contractile dysfunction is cardiomyocyte apoptosis. TUNEL-positive apoptotic myocytes were increased in the heart of *RyR-2*$^{+/-}$ mice compared with WT mice after chronic pressure overload. It has also been indicated that pressure overload-induced cardiac hypertrophy is initiated by a wave of apoptosis of cardiomyocytes, which is involved in the pathogenesis of cardiac remodeling.[37] Because cardiomyocyte apoptosis plays a causal role in contractile dysfunction and HF,[27,32] increased apoptosis of cardiomyocytes may be a potential mechanism of impaired contractility rather than induction of hypertrophy in *RyR-2*$^{+/-}$ mice under hemodynamic overload in the setting. Although the exact mechanism by which apoptosis is increased in the heart of *RyR-2*$^{+/-}$ mice is not clear, it may be because of an indirect mechanism involving attenuated activation of cell survival pathways, such as ERK and Akt. Another possible $Ca^{2+}$-independent mechanism of contractile dysfunction is autophagy, and the extent of autophagy in response to pressure overload was decreased in the heart of *RyR-2*$^{+/-}$ mice compared with WT mice. Autophagy is a highly conserved cellular mechanism of protein recycling that can lead to cell survival or death. The causal role of autophagy in the pathogenesis of cardiac remodeling and HF is controversial,[33,34] and reduced autophagy may simply reflect the attenuated cardiac hypertrophy and impaired cardiac function in the *RyR-2*$^{+/-}$ heart. The

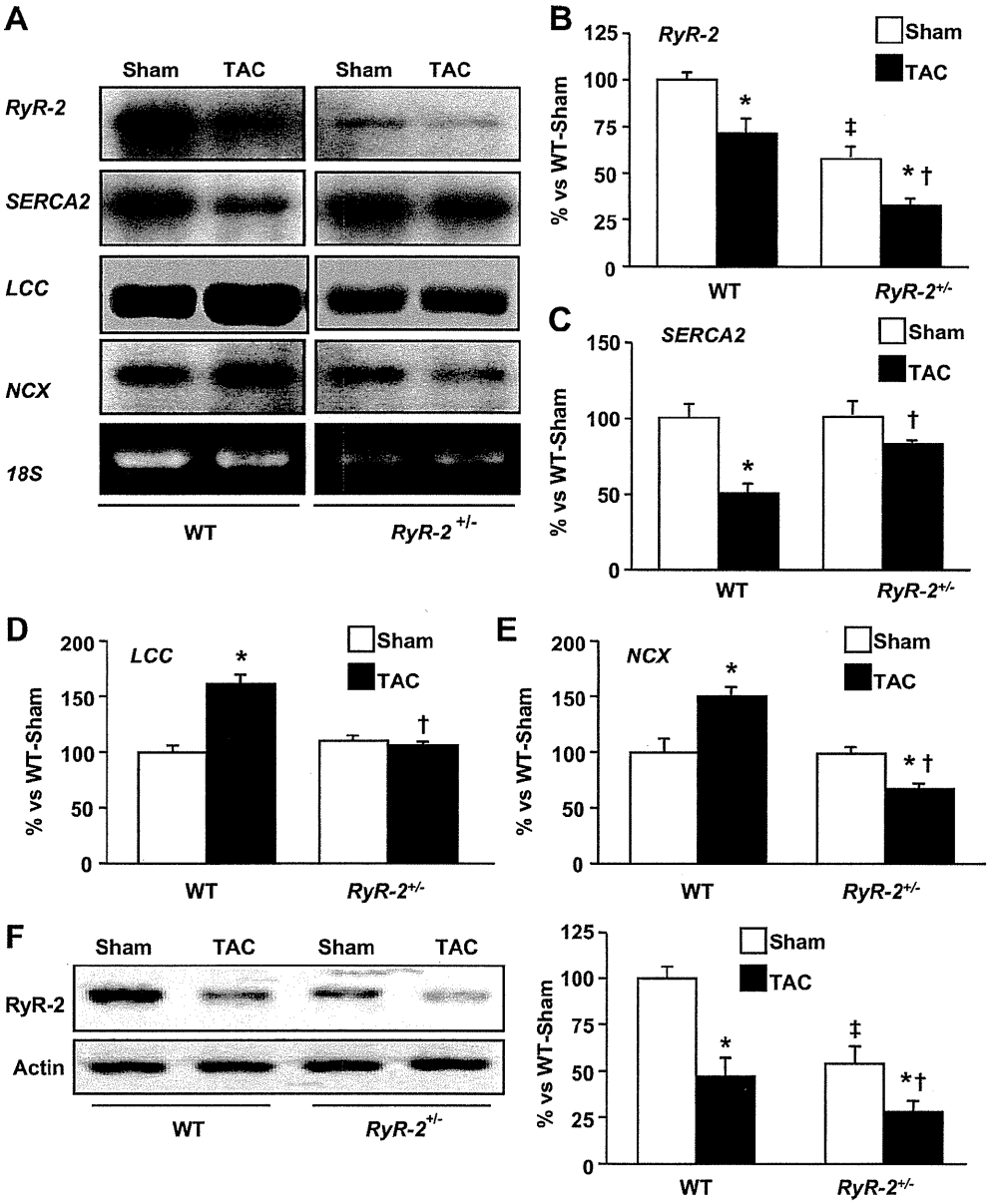


**Figure 5.** Expression of $Ca^{2+}$ handling molecules. **A**, Representative Northern blots. **B** through **E**, Quantitative analyses of the expression levels of *RyR-2*, *SERCA2*, *LCC*, and *NCX* genes. **F**, Western blot analysis for RyR-2 protein expression. Representative blots are shown. The intensities were expressed as percentage of those obtained from wild-type (WT)-sham. Data represent mean±SD from 3 hearts. *$P<0.05$ vs respective sham; †$P<0.05$ vs WT-thoracic aorta constriction (TAC) group; ‡$P<0.05$ vs WT-sham group.

third possible $Ca^{2+}$-independent mechanism of contractile dysfunction is myocardial ischemia.[35,36] It was shown that impaired coronary angiogenesis in the chronic stage of pressure overload contributes to the transition from adaptive to maladaptive cardiac hypertrophy.[27] However, coronary vessel number and the expression of vascular endothelial growth factor in the heart were not altered between WT and *RyR-2*$^{+/-}$ mice, suggesting that this mechanism does not contribute to the impaired contractility of the *RyR-2*$^{+/-}$ heart under chronic overload.

In this study we have also shown that *RyR-2*$^{+/-}$ mice exhibited attenuated cardiac hypertrophy and myocardial fibrosis in response to pressure overload. These were associated with reduced or altered hypertrophic responses of the heart. Van Oort et al[19] have reported recently that, in *RyR-2-R176Q* knockin mice with the defective cardiac RyR-2, pressure overload induced an enhanced hypertrophic response compared with WT mice, which is attributed to an increased SR $Ca^{2+}$ leak and the prohypertrophic CnA/NFAT pathway. In our present study, we observed decreased phosphorylation of CnA in the *RyR-2*$^{+/-}$ heart compared with WT mice under the condition of pressure overload. Although the reason for this difference is not clearly understood, there are several possibilities. At first, mice models are different. We used heterozygous *RyR-2*-knockout mice, whereas Van Oort et al[19] used *RyR-2-R176Q* knockin mice. In *RyR-2*$^{+/-}$ mice, although the expression of RyR-2 is about half decreased and the remained RyR-2 channels are hyperphosphorylated at

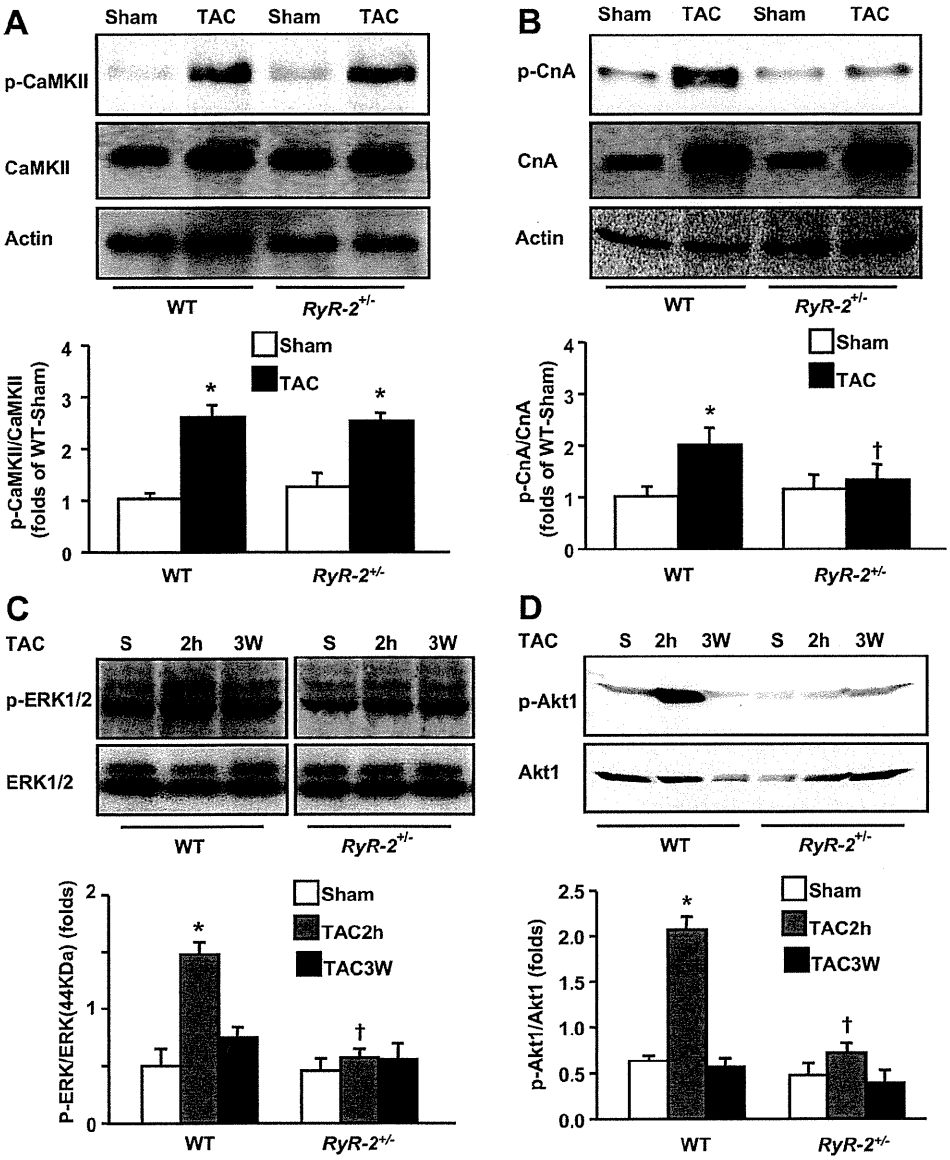


**Figure 6.** Activation of hypertrophic signaling pathways. Total proteins (**A**, **C**, and **D**) or immunoprecipitates with an anti-calcineurin (CnA) antibody (**B**) were analyzed by Western blot analysis. Samples were obtained 3 weeks after the operation (**A** and **B**), or 2 hours (2h) and 3 weeks (3W) after the operation (**C** and **D**). Representative blots showing total and phosphorylated calmodulin-dependent protein kinase II (CaMKII), CnA, extracellular signal-regulated kinase (ERK)1/2, and Akt1 are shown. β-Actin expression served as a loading control for CaMKII and CnA. Phosphorylated CaMKII, CnA, ERK (44 kDa), and Akt1 were expressed as folds of CaMKII, CnA, ERK (44 kDa), and Akt1, respectively. Data represent mean±SD from 3 hearts. *$P<0.05$ vs respective sham; †$P<0.05$ vs corresponding wild-type (WT)-thoracic aorta constriction (TAC) group.

basal condition, the structural, functional, and hemodynamic abnormalities of the heart are not found. In *RyR-2-R176Q* knockin mice, although the structures are normal, there are lower end-diastolic volume and higher end-diastolic pressure compared with WT mice.[38] These differences between the 2 types of mice might contribute to the different results of cardiac hypertrophy. Secondly, the period after TAC is different. We observed pressure overload-induced cardiac hypertrophy within 3 weeks, whereas Van Oort et al[19] showed the results at 8 weeks after TAC. The third one is SR $Ca^{2+}$ leak and activation of CnA. Van Oort et al[19] have demonstrated the increases in SR $Ca^{2+}$ leak and activation of the CnA pathway in *RyR-2-R176Q* knockin mice under TAC condition, whereas we observed a decrease of SR $Ca^{2+}$ release and CnA phosphorylation after TAC in *RyR-2*$^{-/+}$ mice.

Of the 2 major regulators of $Ca^{2+}$-mediated cardiac hypertrophy, CaMKII activation, and its target molecules, HDACs and *MEF2* were comparable between WT and *RyR-2*$^{+/-}$ mice, whereas CnA activation and its target *GATA4* were severely attenuated in the heart of *RyR-2*$^{+/-}$ mice compared with those in WT mice. We have shown previously that CnA activation requires a potent CICR in cardiomyocytes,[25] whereas CaMKII could be activated without increase in intracellular $Ca^{2+}$ (Figure S4), suggesting the possibility that, although reduced CICR in *RyR-2*$^{+/-}$ cardiomyocytes does

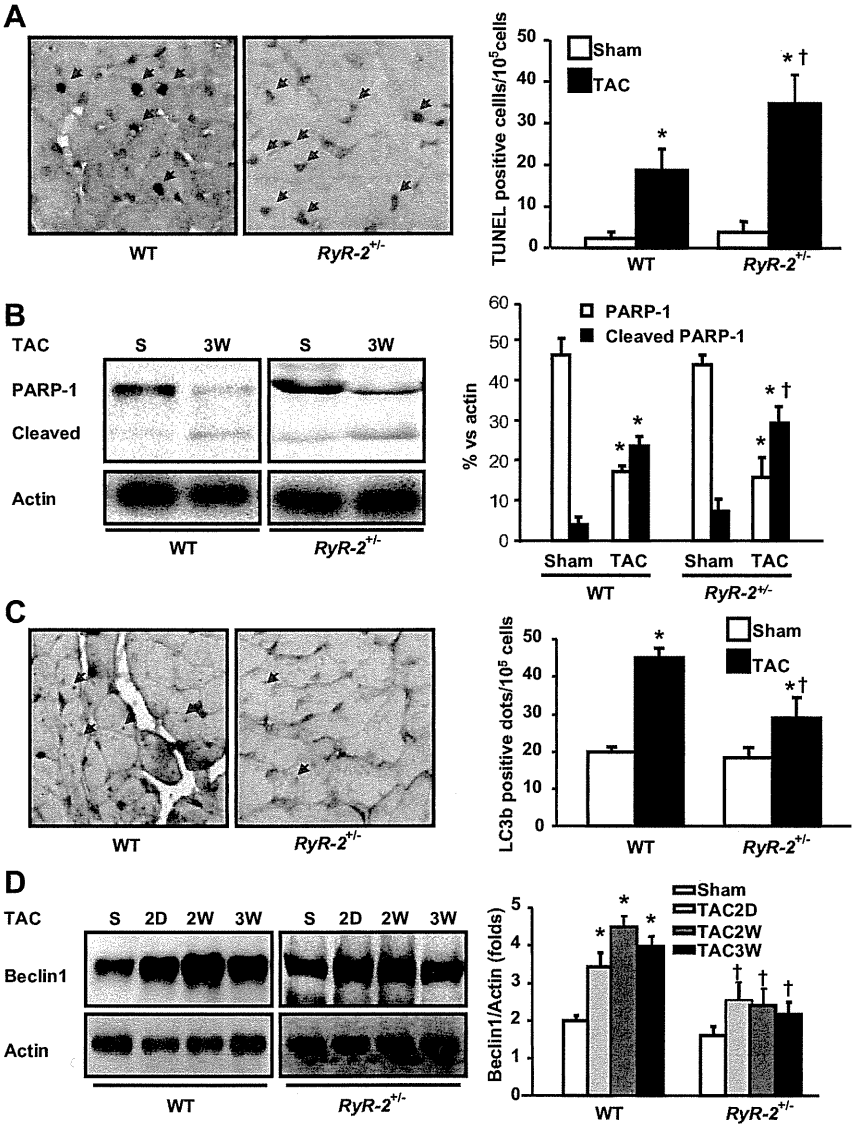


**Figure 7.** Apoptosis and autophagy in myocardium 3 weeks after thoracic aorta constriction (TAC). **A**, Apoptosis. Left ventricular (LV) sections were costained with TUNEL and α-major histocompatibility complex (MHC). Representative photographs are shown. Arrows indicate TUNEL-positive nuclei in α-MHC–stained cells. Apoptosis was evaluated as the number of TUNEL-positive nuclei per $10^5$ cardiomyocytes in the whole LV section. **B**, Western blot analyses for intact poly (ADP-ribose) polymerase-1 (PARP-1) and cleaved PARP-1. β-Actin served as a loading control. Representative blots are shown. The intensities of intact PARP-1 and cleaved PARP-1 were expressed as folds of β-actin. **C**, Autophagy. Representative photographs show double staining against LC3b and α-MHC. Brown dots indicate LC3b-positive aggregates in cardiomyocytes. LC3b-positive aggregates were calculated as the number of LC3b-positive aggregates per $10^5$ cardiomyocytes in LV area. **D**, Western blot analysis for beclin1. Samples were obtained 2 days (2D), 2 weeks (2W), and 3 weeks (3W) after TAC. β-Actin served as a loading control. Representative blots are shown. The intensities of beclin1 were expressed as folds of β-actin. Data represent mean±SD obtained from 5 hearts. $^*P<0.05$ vs respective sham; †$P<0.05$ vs corresponding wild-type (WT)-TAC group.

not affect the CaMKII activity by pressure overload, it contributes to impaired activation of CnA and, therefore, reduced cardiac hypertrophy and fibrosis in *RyR-2*$^{+/-}$ mice. Another possibility is that reduced levels of RyR-2 in the setting of chronic pressure overload induced the altered expression and/or localization of potential mediators of E-C coupling-independent $Ca^{2+}$ entry, leading to impaired activation of $Ca^{2+}$-dependent hypertrophic signaling pathways. Additionally, chronic pressure overload-induced ERK1/2 and Akt activation was also attenuated in the heart of *RyR-2*$^{+/-}$ mice, although the exact mechanisms of downregulation of these signaling pathways are not clear. We reported previously that ERK activation in cardiomyocytes by isoproterenol is mediated by CnA,[25] suggesting that impaired ERK activation in the *RyR-2*$^{+/-}$ heart is attributed to reduced CnA activity. Although it was reported that mitogen-activated protein kinase/extracellular signal-regulated kinase kinase 1-dependent ERK activation in the heart is not attenuated in CnA knockout mice,[39] arguing against the possibility that attenuated CnA activation contributes to impaired ERK activation, our results suggest that activation of ERKs and Akt by pressure overload, at least in part, requires RyR-2–dependent activation of CnA, which associates with myocardial hypertrophy and fibrosis.

We conclude that RyR-2 contributes to the development of cardiac hypertrophy and adaptation of cardiac function during pressure overload through regulation of $Ca^{2+}$ handling. Van Oort et al[19] have demonstrated that the increased $Ca^{2+}$ release through RyR-2 from the SR induces activation of CnA and dephosphorylation and translocation of NFAT3 into the nucleus, thereby inducing hypertrophic gene expression.[19] We speculate here that, other than activation of the CnA/NFAT3 pathway, RyR-2–mediated $Ca^{2+}$ release from the SR induces activation of the CnA/ERKs, Akt, and cardiomyocyte survival pathway, which may also contribute to pressure overload-induced cardiac hypertrophy. Activation of CaMKII and myocardial angiogenesis seems to be not affected by *RyR-2* deficiency.

## Perspectives

By using the *RyR-2*-deficient mice, we have provided direct evidence to demonstrate that, in addition to its

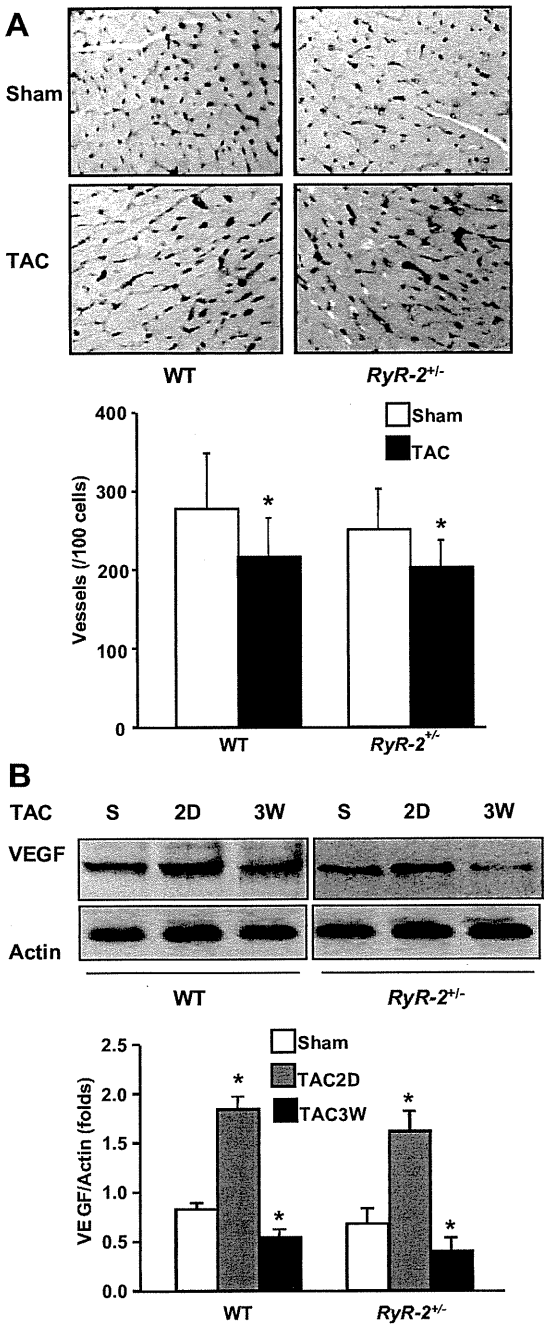


**Figure 8.** Coronary microvessel density and vascular endothelial growth factor (VEGF) expression in the heart. **A**, Coronary microvessel density evaluated by CD31 staining. The number of vessels was counted for 100 cells. **B**, Western blot analysis of VEGF expression. Samples were obtained 2 days (2D) and 3 weeks (3W) after thoracic aorta constriction (TAC). Representative blots are shown. The intensities of VEGF were expressed as folds of β-actin. Data represent mean±SD from 3 hearts. *$P<0.05$ vs respective sham.

well-established role in the regulation of E-C coupling, RyR-2 also regulates cardiac hypertrophy in response to pressure overload. Further elucidation of the exact mechanisms of RyR-2–mediated cardiac hypertrophy will lead to the in-depth understanding of cardiac hypertrophy and HF.

## Sources of Funding

This work was supported by the grants from the National Natural Science Foundation of China (30525018 and 30971250) and National Basic Research Program of China (2007CB512003; to Y.Z.) and by a Grant-in-Aid for Scientific Research, Developmental Scientific Research, and Scientific Research on Priority Areas from the Ministry of Education, Science, Sports, and Culture of Japan (to I.K.).

## Disclosures

None.

## References

1. Frey N, Olson EN. Cardiac hypertrophy: the good, the bad, and the ugly. *Annu Rev Physiol.* 2003;65:45–79.
2. Chien KR. Stress pathways and heart failure. *Cell.* 1999;98:555–558.
3. Stuyvers BD, Boyden PA, ter Keurs HEDJ. Calcium waves: physiological relevance in cardiac function. *Circ Res.* 2000;86:1016–1018.
4. Carafoli E. Calcium signaling: a tale for all seasons. *Proc Natl Acad Sci U S A.* 2002;99:1115–1122.
5. Bers DM. Calcium fluxes involved in control of cardiac myocytes contraction. *Circ Res.* 2000;87:275–281.
6. Bers DM. Calcium cycling and signaling in cardiac myocytes. *Annu Rev Physiol.* 2008;70:23–49.
7. Muth JN, Body I, Lewis W, Varadi G, Schwartz A. A $Ca^{2+}$-dependent transgenic model of cardiac hypertrophy: a role for protein kinase Cα. *Circulation.* 2001;103:140–147.
8. Yamazaki T, Komuro I, Zou Y, Kudoh S, Shiojima I, Mizuno T, Hiroi Y, Nagai R, Yazaki Y. Efficient inhibition of the development of cardiac remodeling by a long-acting calcium antagonist amlodipine. *Hypertension.* 1998;31:32–38.
9. Zou Y, Yamazaki T, Nakagawa K, Yamada H, Iriguchi N, Toko H, Takano H, Akazawa H, Nagai R, Komuro I. Continuous blockade of L-type $Ca^{2+}$ channels suppresses activation of calcineurin and development of cardiac hypertrophy in spontaneously hypertensive rats. *Hypertens Res.* 2002;25:117–124.
10. Ji Y, Lalli MJ, Babu GJ, Xu Y, Kirkpatrick DL, Liu LH, Chiamvimonvat N, Walsh RA, Shull GE, Periasamy M. Disruption of a single copy of the SERCA2 gene results in altered $Ca^{2+}$ homeostasis and cardiomyocyte function. *J Biol Chem.* 2000;275:38073–38080.
11. Andersson KB, Birkeland JA, Finsen AV, Louch WE, Sjaastad I, Wang Y, Chen J, Molkentin JD, Chien KR, Sejersted OM, Christensen G. Moderate heart dysfunction in mice with inducible cardiomyocyte-specific excision of the SERCA2 gene. *J Mol Cell Cardiol.* 2009;47:180–187.
12. Hobai IA, O'Rourke B. The potential of $Na^+/Ca^{2+}$ exchange blockers in the treatment of cardiac disease. *Expert Opin Investig Drugs.* 2004;13:653–664.
13. Takimoto E, Yao A, Toko H, Takano H, Shimoyama M, Sonoda M, Wakimoto K, Takahashi T, Akazawa H, Mizukami M, Nagai T, Nagai R, Komuro I. Sodium calcium exchanger plays a key role in alteration of cardiac function in response to pressure overload. *FASEB J.* 2002;16:373–378.
14. Hasenfuss G, Pieske B. Calcium cycling in congestive heart failure. *J Mol Cell Cardiol.* 2002;34:951–969.
15. Yano M, Ikeda Y, Matsuzaki M. Altered intracellular $Ca^{2+}$ handling in heart failure. *J Clin Invest.* 2005;115:556–564.
16. Wehrens XH, Lehnart SE, Marks AR. Intracellular calcium release and cardiac disease. *Annu Rev Physiol.* 2005;67:69–98.
17. Marks AR. Ryanodine receptors, FKBP12, and heart failure. *Front Biosci.* 2002;7:d970–d977.
18. Zhao L, Sebkhi A, Nunez DJ, Long L, Haley CS, Szpirer J, Szpirer C, Williams AJ, Wilkins MR. Right ventricular hypertrophy secondary to pulmonary hypertension is linked to rat chromosome 17: evaluation of cardiac ryanodine RyR-2 receptor as a candidate. *Circulation.* 2001;103:442–447.
19. Van Oort RJ, Respress JL, Li N, Reynolds C, De Almeida AC, Skapura DG, De Windt LJ, Wehrens XHT. Accelerated development of pressure overload-induced cardiac hypertrophy and dysfunction in an RyR2–R176Q knockin mouse model. *Hypertension.* 2010;55:932–938.
20. Houser SR, Molkentin JD. Does contractile $Ca^{2+}$ control calcineurin-NFAT signaling and pathological hypertrophy in cardiac myocytes? *Sci Signal.* 2008;1:pe31.

21. Molkentin JD. Dichotomy of $Ca^{2+}$ in the heart: contraction versus intracellular signaling. *J Clin Invest.* 2006;116:623–626.
22. Backs J, Olson EN. Control of cardiac growth by histone acetylation/deacetylation. *Circ Res.* 2006;98:15–24.
23. Heineke J, Molkentin JD. Regulation of cardiac hypertrophy by intracellular signalling pathways. *Nat Rev Mol Cell Biol.* 2006;7:589–600.
24. Marks AR. Calcium and the heart: a question of life and death. *J Clin Invest.* 2003;111:597–600.
25. Zou Y, Yao A, Zhu W, Kudoh S, Hiroi Y, Shimoyama M, Uozumi H, Kohmoto O, Takahashi T, Shibasaki F, Nagai R, Yazaki Y, Komuro I. Isoproterenol activates extracellular signal-regulated protein kinases in cardiomyocytes through calcineurin. *Circulation.* 2001;104:102–108.
26. Takeshima H, Komazaki S, Hirose K, Nishi M, Noda T, Iino M. Embryonic lethality and abnormal cardiac myocytes in mice lacking ryanodine receptor type 2. *EMBO J.* 1998;17:3309–3316.
27. Sano M, Minamino T, Toko H, Miyauchi H, Orimo M, Qin Y, Akazawa H, Tateno K, Kayama Y, Harada M, Shimizu I, Asahara T, Hamada H, Tomita S, Molkentin JD, Zou Y, Komuro I. p53-induced inhibition of Hif-1 causes cardiac dysfunction during pressure overload. *Nature.* 2007;446:444–448.
28. Wu J, Bu L, Gong H, Jiang G, Li L, Ma H, Zhou N, Lin L, Chen Z, Ye Y, Niu Y, Sun A, Ge J, Zou Y. Effects of heart rate and anesthetic timing on high-resolution echocardiographic assessment under isoflurane anesthesia in mice. *J Ultrasound Med.* 2010;29:1771–1778.
29. Yao A, Su Z, Nonaka A, Nonaka A, Zubair I, Lu L, Philipson KD, Bridge JHB, Barry WH. Effects of overexpression of the $Na^{+}$-$Ca^{2+}$ exchanger on $[Ca^{2+}]i$ transients in murine ventricular myocytes. *Circ Res.* 1998;82:657–665.
30. Zou Y, Hiroi Y, Uozumi H, Takimoto E, Toko H, Zhu W, Kudoh S, Mizukami M, Shimoyama M, Shibasaki F, Nagai R, Yazaki Y, Komuro I. Calcineurin plays a critical role in the development of pressure overload-induced cardiac hypertrophy. *Circulation.* 2001;104:97–101.
31. Hoshijima M, Chien KR. Mixed signals in heart failure: cancer rules. *J Clin Invest.* 2002;109:849–855.
32. Foo RS, Mani K, Kitsis RN. Death begets failure in the heart. *J Clin Invest.* 2005;115:565–571.
33. Rothermel BA, Hill JA. Autophagy in load-induced heart disease. *Circ Res.* 2008;103:1363–1369.
34. Nishida K, Yamaguchi O, Otsu K. Crosstalk between autophagy and apoptosis in heart disease. *Circ Res.* 2008;103:343–351.
35. Dorn GW, II. Myocardial angiogenesis: its absence makes the growing heart founder. *Cell Metab.* 2007;5:326–327.
36. Walsh K, Shiojima I. Cardiac growth and angiogenesis coordinated by intertissue interactions. *J Clin Invest.* 2007;117:3176–3179.
37. Teiger E, Than VD, Richard L, Wisnewsky C, Tea BS, Gaboury L, Tremblay J, Schwartz K, Hamet P. Apoptosis in pressure overload-induced heart hypertrophy in the rat. *J Clin Invest.* 1996;97:2891–2897.
38. Kannankeril PJ, Mitchell BM, Goonasekera SA, Chelu MG, Zhang W, Sood S, Kearney DL, Danila CI, Biasi MD, Wehrens XHT, Pautler RG, Roden DM, Taffet GE, Dirksen RT, Anderson ME, Hamilton SL. Mice with the R176Q cardiac ryanodine receptor mutation exhibit catecholamine-induced ventricular tachycardia and cardiomyopathy. *Proc Natl Acad Sci U S A.* 2006;103:12179–12184.
39. Sanna B, Bueno OF, Dai YS, Wilkins BJ, Molkentin JD. Direct and indirect interactions between calcineurin-NFAT and MEK1-extracellular signal-regulated kinase 1/2 signaling pathways regulate cardiac gene expression and cellular growth. *Mol Cell Biol.* 2005;25:865–878.

**Online Data Supplement**

# Ryanodine receptor type 2 is required for the development of pressure overload-induced cardiac hypertrophy

Yunzeng Zou [1], Yanyan Liang [1], Hui Gong [1], Ning Zhou [1], Hong Ma [1, 7], Aili Guan [1], Aijun Sun [1], Ping Wang [2], Yuhong Niu [1], Hong Jiang [1], Hiroyuki Takano [2], Haruhiro Toko [2], Atsushi Yao [3], Hiroshi Takeshima [4], Hiroshi Akazawa [5], Ichiro Shiojima [5], Yuqi Wang [6], Issei Komuro [5], Junbo Ge [1]

[1] Shanghai Institute of Cardiovascular Diseases, Zhongshan Hospital and Institutes of Biomedical Sciences, Fudan University, Shanghai, China;
[2] Department of Cardiovascular Science and Medicine, Chiba University Graduate School of Medicine, Chiba, Japan
[3] Department of Cardiovascular Medicine, University of Tokyo Graduate School of Medicine, Tokyo, Japan;
[4] Department of Biochemistry, Tohoku University Graduate School of Medicine, Sentai, Japan
[5] Department of Cardiovascular Medicine, Osaka University Graduate School of Medicine, Osaka, Japan;
[6] Department of Vascular Surgery, Zhongshan Hospital, Fudan University, Shanghai, China
[7] Department of Cardiology, Second Affiliated Hospital, Zhejiang University College of Medicine, Hangzhou, China,

*Correspondence to:
Yunzeng Zou, MD, PhD,
Shanghai Institute of Cardiovascular Diseases, Zhongshan Hospital and Institutes of Biomedical Sciences, Fudan University,
180 Feng Lin Road, Shanghai 200032, China,
TEL/FAX: +86-21-5423-7969;
Email: zou.yunzeng@zs-hospital.sh.cn